# *High Mass Flow, Ceramic Ram Jet Burner*

*by Henry H. Hicks, Jr. and Alexander Weir, Jr.*

*Project MX-772*
*USAF Contract W33-038-ac-21100*

*Willow Run Research Center*
*Engineering Research Institute*
*University of Michigan*
*UMM-73. December 1950*

## FOREWORD

This report was prepared by the University of Michigan, Engineering Research Institute. The experimental work described here has been done as part of a program of combustion research under E. R. I. Project No. M772 and AF contract W33-038-ac-21100 with Mr. Richard B. Morrison acting as group supervisor and Messrs. E. T. Vincent and J. W. Luecht acting as faculty supervisors for the University of Michigan. The work was administered under the direction of the Fuels and Lubricants Division, Power Plant Laboratory, Engineering Division, Air Materiel Command. This is the initial formal report on this subject. However, some information has been included in earlier progress reports of this project.

ABSTRACT

It is believed that a new approach to ramjet combustion chamber design has been found. Ceramic lined combustion chambers have been made which are capable of handling high flow rates of fuel air mixture without blowout and which can burn such mixtures with high combustion efficiency. Previous work with ceramic lined combustion chambers has apparently considered their thermal resistance only, and not their flameholding ability. The burners used here consist essentially of a cylindrical metal pipe lined with a high refractory materiel. Conventional flame holders or other flow obstructions were not used. Burners have been operated at mass velocities greater than 50 lbs/sec per sq. ft. of combustion chamber cross-sectional area with a combustion efficiency of over 90%. This is considerably greater mass velocity than the mass velocity (30 lbs/sec per sq. ft.) which is required to obtain thermal choking (Mach = 1 at the exit). It is anticipated that this mass velocity can be increased without causing blowout to occur, since the maximum flow rate was limited by the capabilities of the air supply.

TABLE OF CONTENTS

LIST OF ILLUSTRATIONS AND CHARTS

## I. INTRODUCTION

At the present time, certain operational difficulties prevent full realization of the potentialities of the ramjet. Most of these operational difficulties are found in the combustion chamber section of the ramjet and include such items as blowout at high mass flows, rough burning, inefficient combustion, and other problems connected with altitude operation. The Propulsion and Combustion Laboratory at the University of Michigan has investigated, on a basic level, some number of problems connected with ramjet combustion in the past few years. During the course of these investigations, it was found that a ceramic lined combustion chamber containing no flame holder, could be operated efficiently at high mass velocities without blowing out. It is the purpose of this paper to describe this ceramic burner which seems to have marked advantages over the conventional ramjet burners now in use.

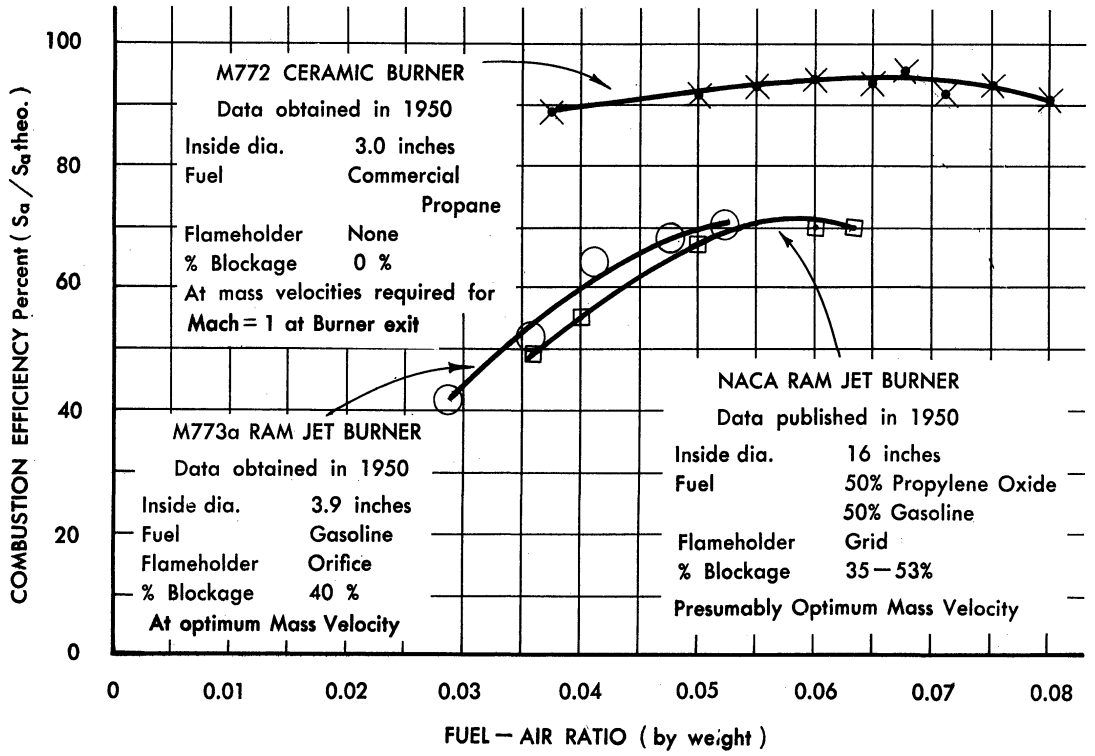


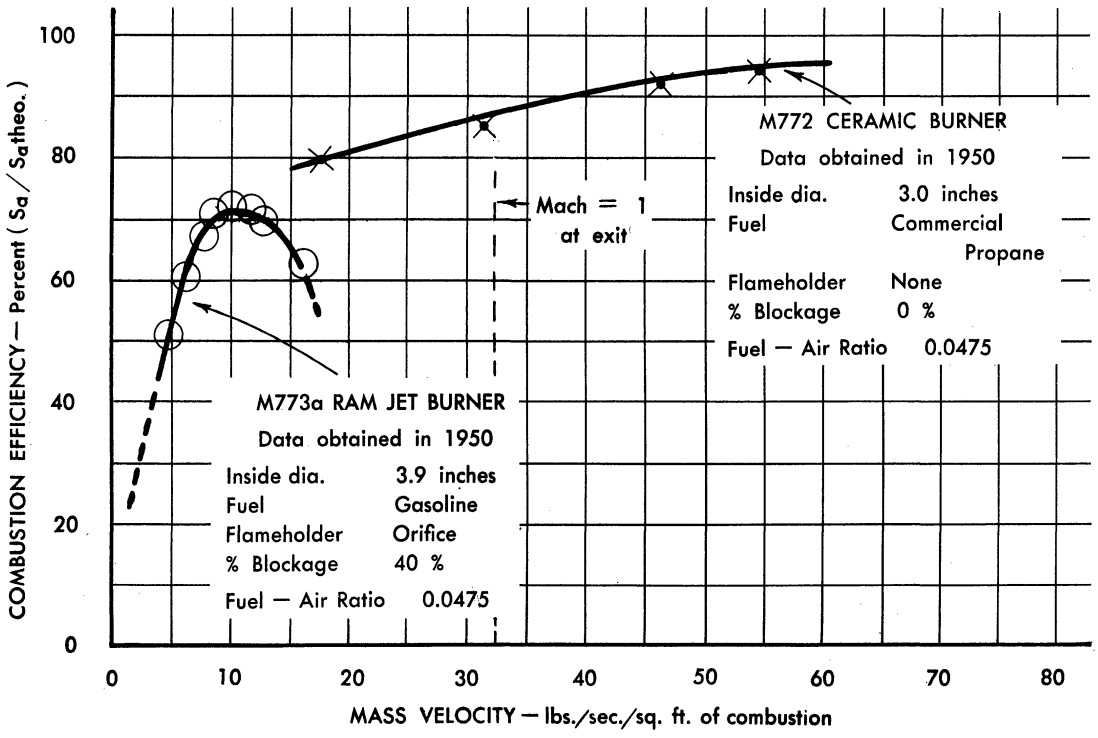


**FIG. 1 COMPARISON OF COMBUSTION EFFICIENCY OF CERAMIC BURNER WITH CONVENTIONAL BURNER**

## II. BURNER PERFORMANCE

The ceramic lined combustion chambers described herein differ from conventional ramjet burners in several ways. One principal difference is that no flame holders are used. Detailed descriptions of the various burners used will be described in another section of this report, but the burners are essentially metal cylinders lined with a high refractory material. The ability of the ceramic burner to handle high mass flows at high efficiency without blowout has been established. Because of this, its use as a propulsion device seems quite attractive, particularly for ramjets.

Some desirable characteristics of combustion chambers include long life, high efficiency, stable operation over a wide range of mass flows, low internal drag, freedom from blowout, as well as ease of fabrication and use of non-critical materials. The ceramic burner developed at the University of Michigan is believed to combine most of these characteristics to a greater degree than any other burner known about here.

The operating temperature is about 3000°F for the ceramic parts of the burner and there are a large number of ceramic materials which will withstand long usage at this temperature provided the stresses are not too high. Ceramics may also be considered non-strategic materials for the most part. At any rate, the materials used in this burner are available in good supply in this country, and the techniques of working with ceramics are a well developed art. It should be noted, however, that the particular ceramic materials used in the University of Michigan combustion chambers are not considered to be totally satisfactory, and further experience may indicate that some other materials will give better results.

It should also be noted that the ceramic materials are not used solely for their heat resisting ability, as has been the case with other ceramic lined combustion chambers, but are used because of the flame holding ability of the hot ceramic surface. A comparison of this burner with conventional ramjet burners will illustrate this point. In figure 1, a plot of combustion efficiency plotted against fuel-air ratio is shown. It may be seen from this that the ceramic burner is operable over a wider range of fuel-air ratios than are the two conventional ramjet burners and is considerably more efficient, being over 90% as compared to a maximum of about 70% for the conventional ramjet burners. In the lower section of figure 1, the combustion efficiency is plotted against the mass

velocity (which is related to the thrust per unit area) and as may be seen, the ceramic burner is operable at mass velocities approximately four times the maximum mass velocity at which the conventional burner would operate. As a matter of fact, the ceramic burner has not been blown out when burning stoichiometric mixtures. The maximum flow rate has been limited by the capabilities of the air supply.

The efficiency of a combustion chamber may be expressed in various ways, and may mean different things to different people. Herein by efficiency is meant the effectiveness of the burner to turn the potential chemical energy of the fuel-air mixture into momentum of the ejected combustion products. The percentage of the maximum theoretical momentum that is actually attained is the burner efficiency.

A convenient criteria for expressing performance in the above way has been the $S_a$ term used here[1] and elsewhere. For a given inlet condition there is a theoretical maximum $S_a$ and of which the actual value of $S_a$ of the burner can be expressed as a percentage. This gives a performance analysis based on $S_a$. In figure 1, therefore, the combustion efficiences are the percentage of the maximum $S_a$ obtainable (i.e. 100 x $S_a$ actual/$S_a$ theoretical).

One of the most interesting points about the ceramic burner is that extremely high mass flows can be handled in a small unit. The ceramic burner has been operated to liberate about forty times as many BTU/sec/cu ft of combustion chamber volume as is obtained in a conventional turbojet combustion can. As far as a practical application may be concerned, a small burner size would allow more space for fuel, instruments, etc., but probably of more importance is the condition that a reduction in size will allow a reduction in weight. The fact that operation can be carried on at high mass velocities (Mach = 1 at exit) means that a contracting section is not needed at the exit of the ramjet and that under certain conditions an expansion nozzle would be used.

## III. DESCRIPTION OF EQUIPMENT

### A. Combustion Chambers

The combustion chambers used in these experiments are essentially metal tubes into which ceramic refractory liners have been placed. The configuration and the material of the liner have an important bearing on the performance of the chamber. The first ceramic burner tested was lined with a diaspore clay firebrick obtained from the Massillon Refractories Company.* A cross-sectional view of this burner (Burner No. 1) is shown in figure 2. Preliminary tests were made with this burner before Burner No. 2 was constructed. Burner No. 1 was 18 in. long and had an inside diameter of 2.00 in. The outside of the refractory material was retained by a piece of 4 in. Schedule 40 pipe. The refractory material used had a very porous surface, and was used because it was available in the laboratory at that time. Burner No. 2 was constructed of ceramic saggers** obtained from the Champion Spark Plug Company, Detroit, Michigan. These saggers were used because they were readily obtainable, and not necessarily because of their special shape or refractory properties. The saggers were made of a high alumina content material, the surface having less porosity than the surface of Burner No. 1. The dimensions of Burner No. 2 are shown in figure 3. Figures 4 and 5 show photographs of this burner in operation. The 0.0625 in. thick stainless steel (18-8) retaining wall on this burner failed, however, probably because of cracks in the cement used to hold the ceramic saggers in place in the 6 in. tubing.

The burners used to obtain the experimental data presented in this report had the dimensions of Burner No. 3 shown in figure 6. Burner lengths of 12, 15, 18, 24, and 30 in. were tested. The ceramic rings used to build up the chamber lining for these burners were manufactured for the purpose by the Massillon Refractories Company, and have a high alumina composition. The retaining tube used for Burner No. 3 was Schedule 40, 5 in. low carbon steel pipe. The surface porosity of

* Massillon Refractories Company, Massillon, Ohio.

** Small refractory containers used in the spark plug manufacturing process.

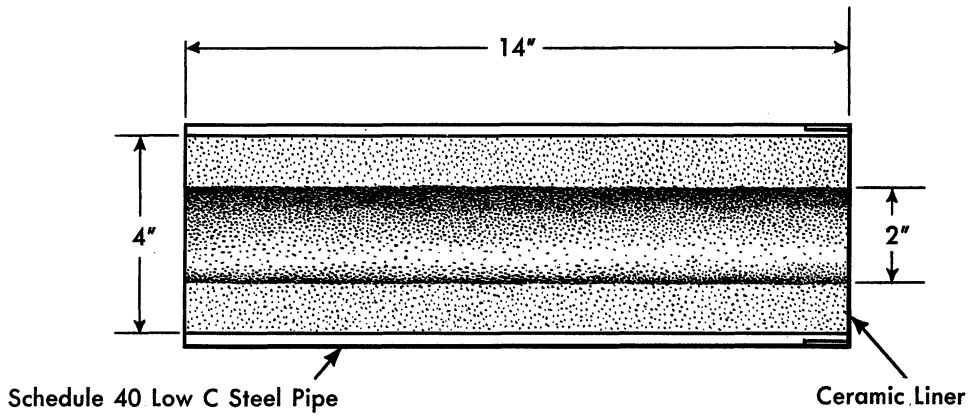


FIG. 2 CERAMIC BURNER No. 1

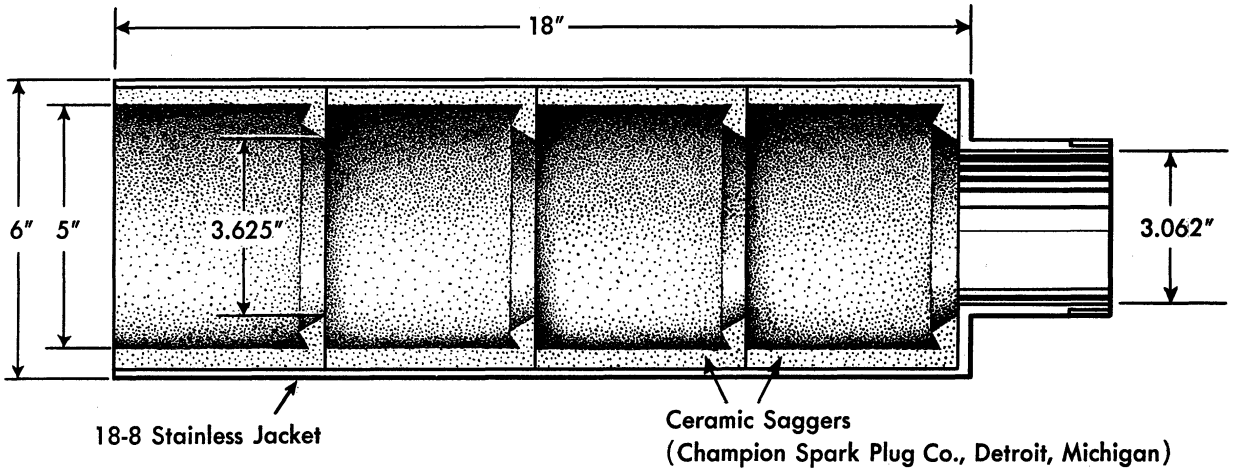


FIG. 3 CERAMIC BURNER No. 2

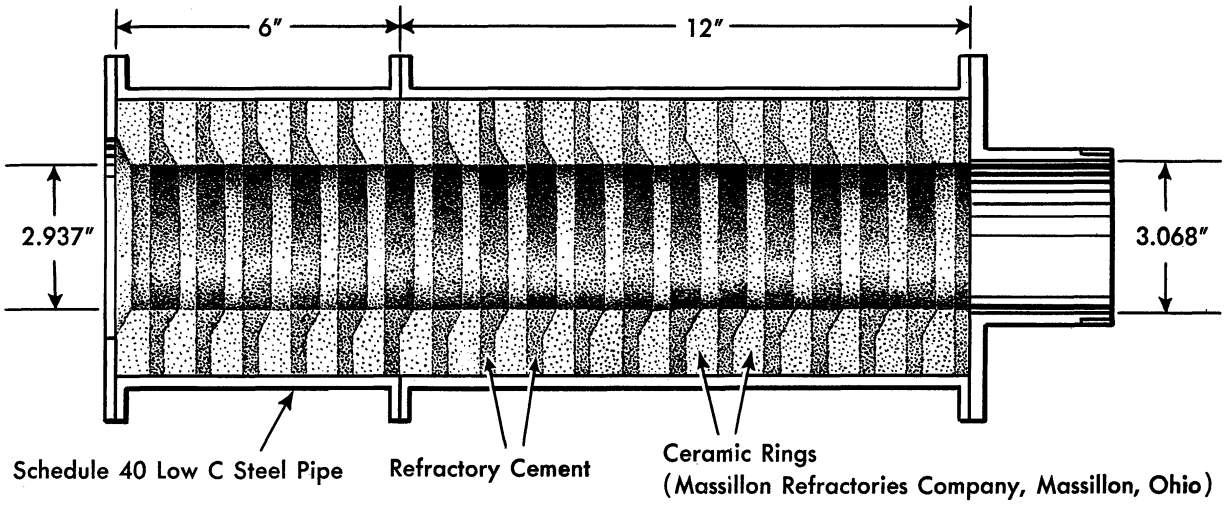


FIG. 4 CERAMIC BURNER No. 3

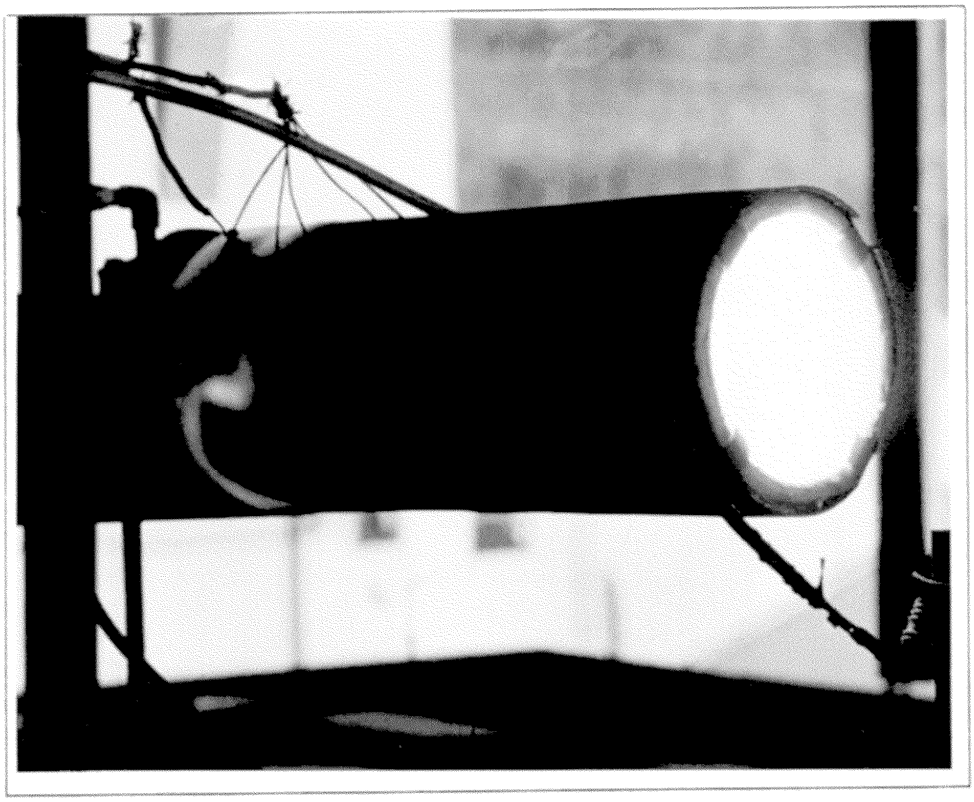

FIG. 5 BURNER No. 2 IN OPERATION

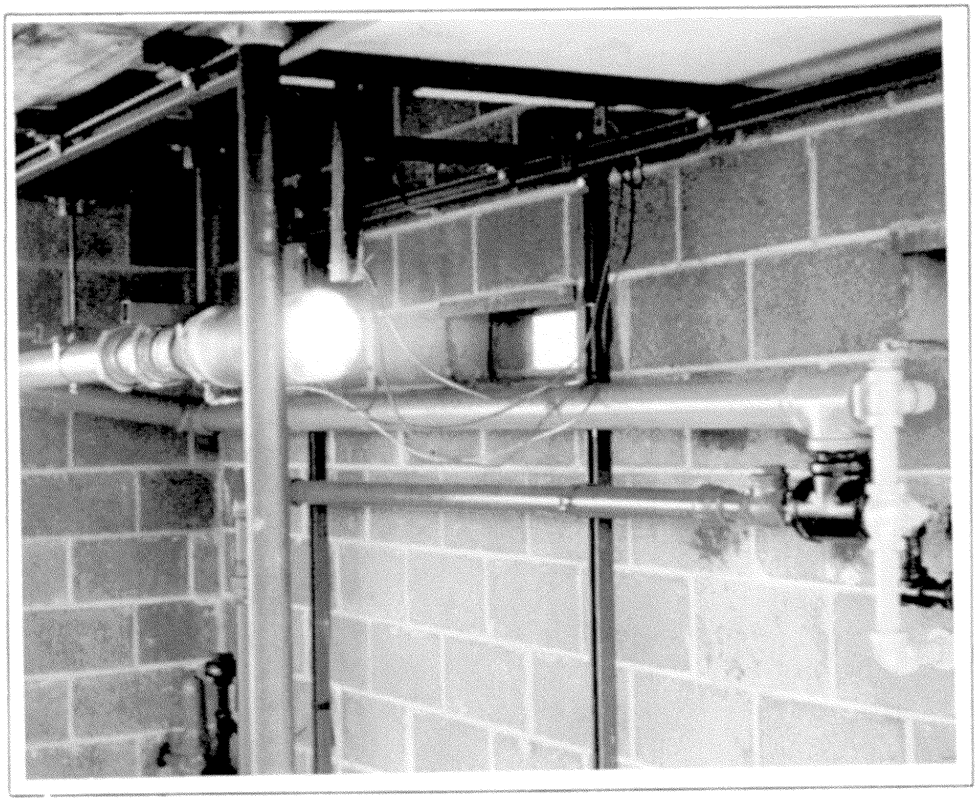

FIG. 6 BURNER VIEWED THROUGH TEST STAND OBSERVATION WINDOW

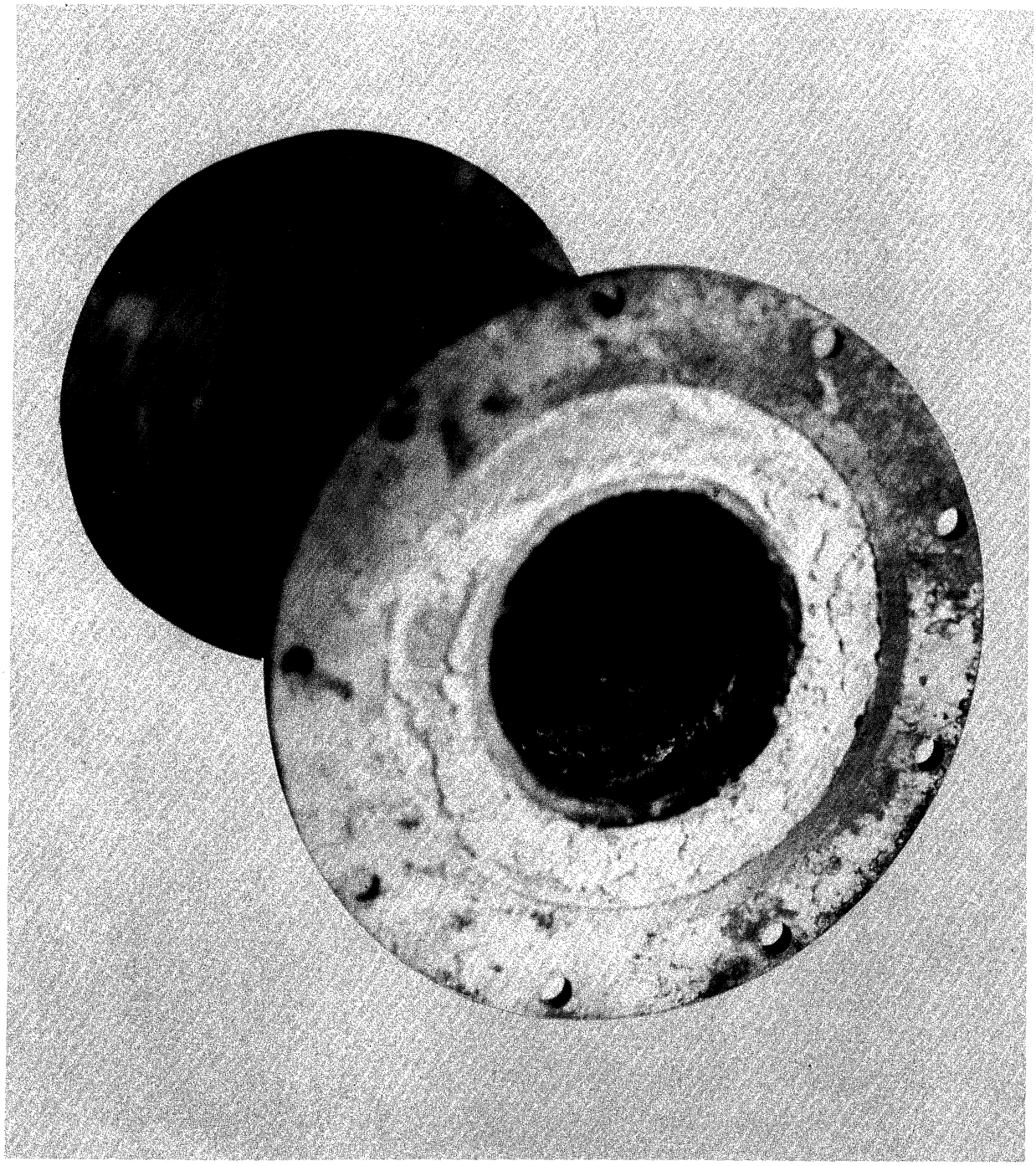

FIG. 7 3 INCH BURNER SECTION

Burner No. 3 was intermediate between that of Burner No. 1 and Burner No. 2. A photograph of a 12 in. section of one of these burners is shown in figure 7.

## B. Facilities

### 1. Air Supply

The air used in the operation is obtained by pressurizing two 80 cu. ft. tanks to 2500 psi and then blowing the tanks down to a pressure of 500 psi, hence obtaining a large flow rate of air* for a short period of time. The tanks are pressurized by means of two 3500 psi discharge pressure Ingersoll-Rand compressors of 70 cfm free air capacity each. The compressors are driven by Waukesha engines which were converted to operate on gaseous propane. Figure 8 is a photograph of the two compressors and the air storage tanks, while Figure 9 shows the compressor shed as constructed and the air tanks. At a flow rate of 10 lbs/sec of air there is sufficient air in the tanks to allow operation for approximately three minutes, with the tank pressure going from 2500 to 500 psi. (The tanks were designed for a working pressure 3500 psi, were hydraulically tested to 5000 psi by the manufacturer, and hydraulically tested to 4000 psi in this laboratory. They have occasionally been operated at 3500 psi but for normal operation, the maximum pressure used is generally 2500 psi.) There is a 1 in. control valve in the low pressure (i.e., 500 psi) section of the 3 in. air line which has restricted the maximum flow to approximately 3 lbs./sec. This valve will be replaced with a larger valve in the near future. Figure 10 is a drawing of the air supply system, showing the pebble type heat exchanger in the foreground which can be used to supply compressed air heated to 1000°F for testing purposes.

### 2. Propane Supply

The fuel used in these experiments was commercial propane obtained from the Phillips Petroleum Company** and specified to contain at least 95% propane or propylene. An oral assurance was given that the

---

* The high charging pressures in the storage tanks causes the air to be very dry.

** Phillips Petroleum Company, Pontiac, Michigan

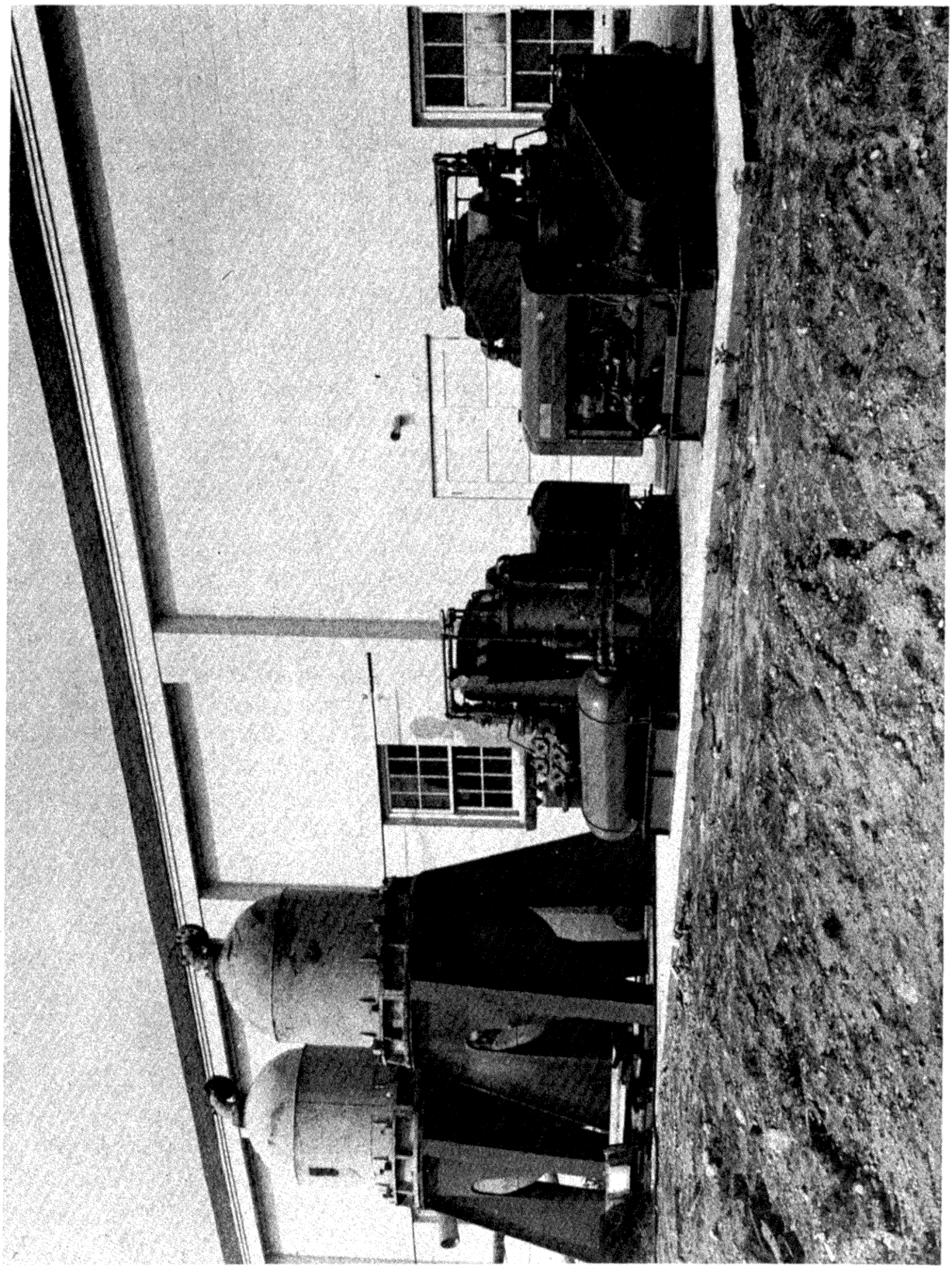

FIG. 8 AIR SUPPLY TANKS AND COMPRESSORS

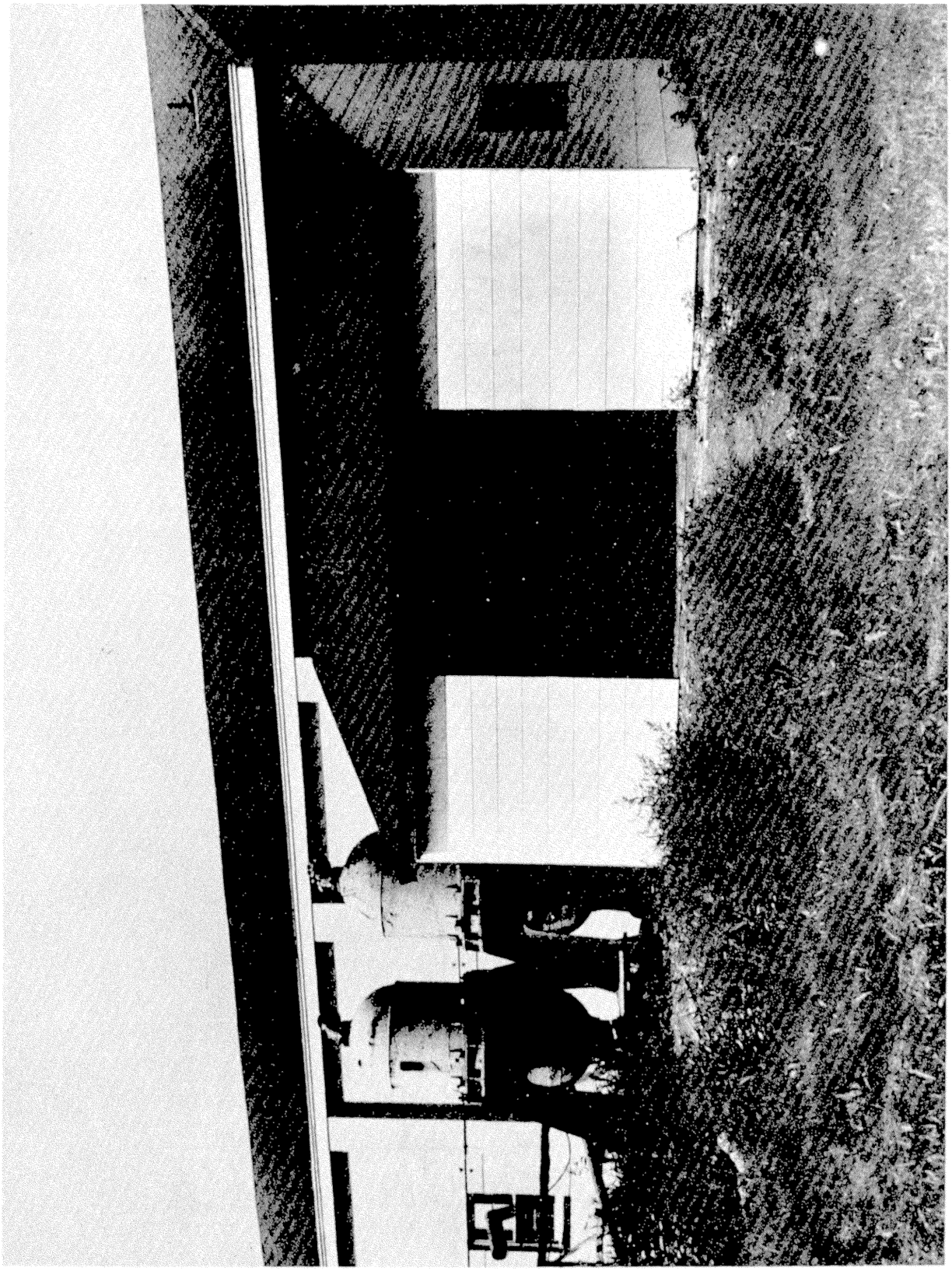

FIG. 9 AIR COMPRESSOR SHED AND TANKS

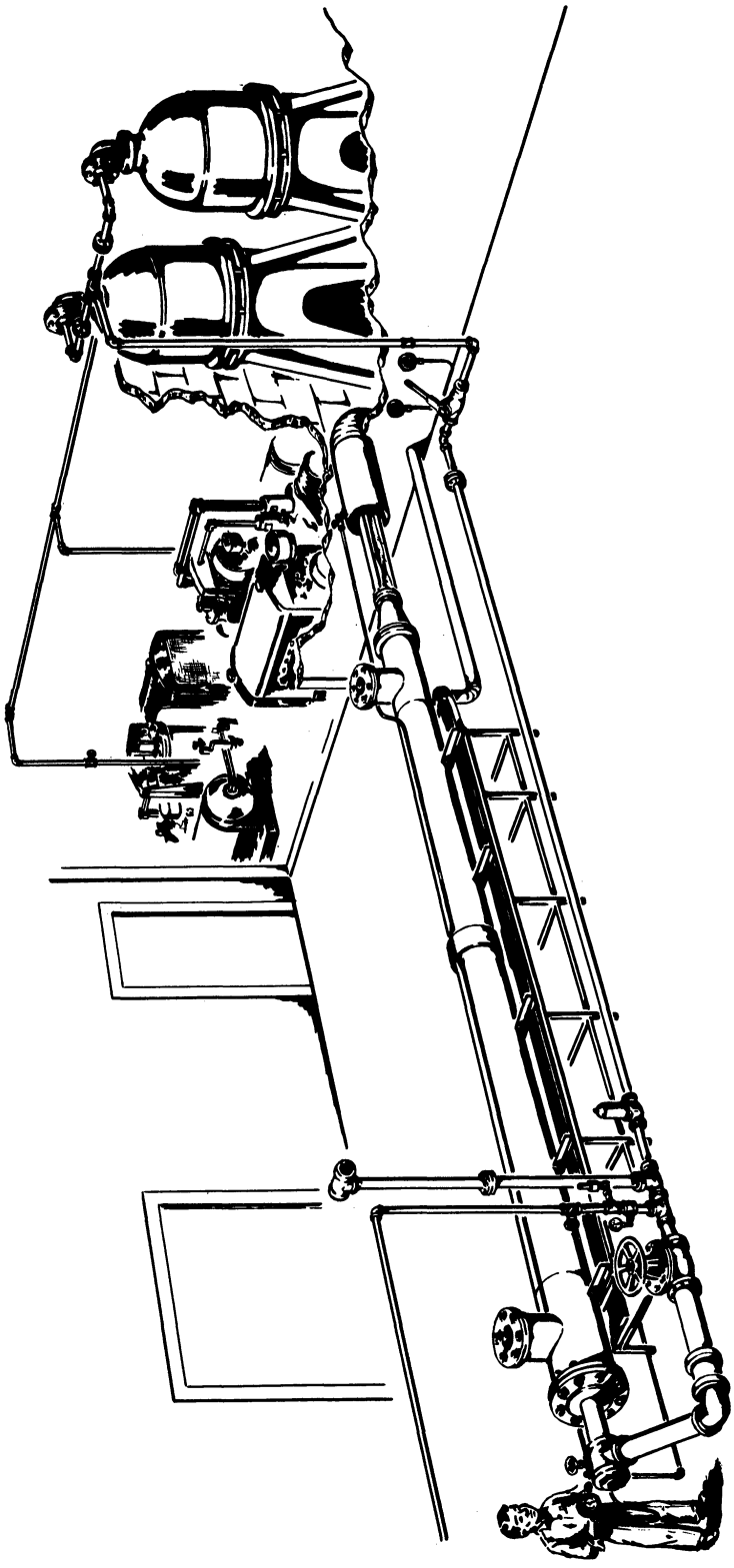

FIG. 10 CUTAWAY VIEW SHOWING TEST EQUIPMENT

propylene content of the various batches of fuel received was small. The fuel was not analyzed. The propane is stored in a 1200 gallon tank located about 200 feet from the test stand. A 2 inch line containing gaseous propane was installed from the supply tank to the test stand. If there were no cooling of propane in the tank due to the latent heat of evaporation, it would be possible to obtain a flow rate of 1 lb/sec for about 70 minutes (the tank is filled with 1000 gallons). Actually, because of the refrigerating effect of the evaporating propane, the operation limit is nearer 30 minutes at this high flow rate, which, however, is quite adequate because of the limitations on the air supply.

### 3. Test Stand

Photographs of the test stand with the burner in operation are shown in figures 11 and 12. Figure 13 is an interior view of the test stand showing the control valves, instruments panel, and observation window.

## C. Instrumentation

### 1. Air Flow

The air flow was metered with a 2.25 inch diameter flat plate square edge orifice constructed of brass and designed according to ASME specifications[2]. Radius taps (i.e., static pressure holes located 1 pipe diameter upstream and 1/2 pipe diameter downstream from the orifice plate) were used. The orifice upstream pressure was maintained at a constant pressure of 500 psi by means of a 1 inch Foster Reducing Valve. The upstream pressure and downstream temperature of the air was measured with indicating gages located inside the control cell, while the pressure drop across the orifice was measured with a water manometer.

### 2. Propane Flow

The propane flow was metered with a 0.890 inch diameter flat plate orifice constructed according to ASME Specifications[2]. Radius taps were used and the upstream pressure, downstream temperature and pressure drop (across orifice) were measured. The upstream pressure at the orifice was equal to the vapor pressure of the propane under

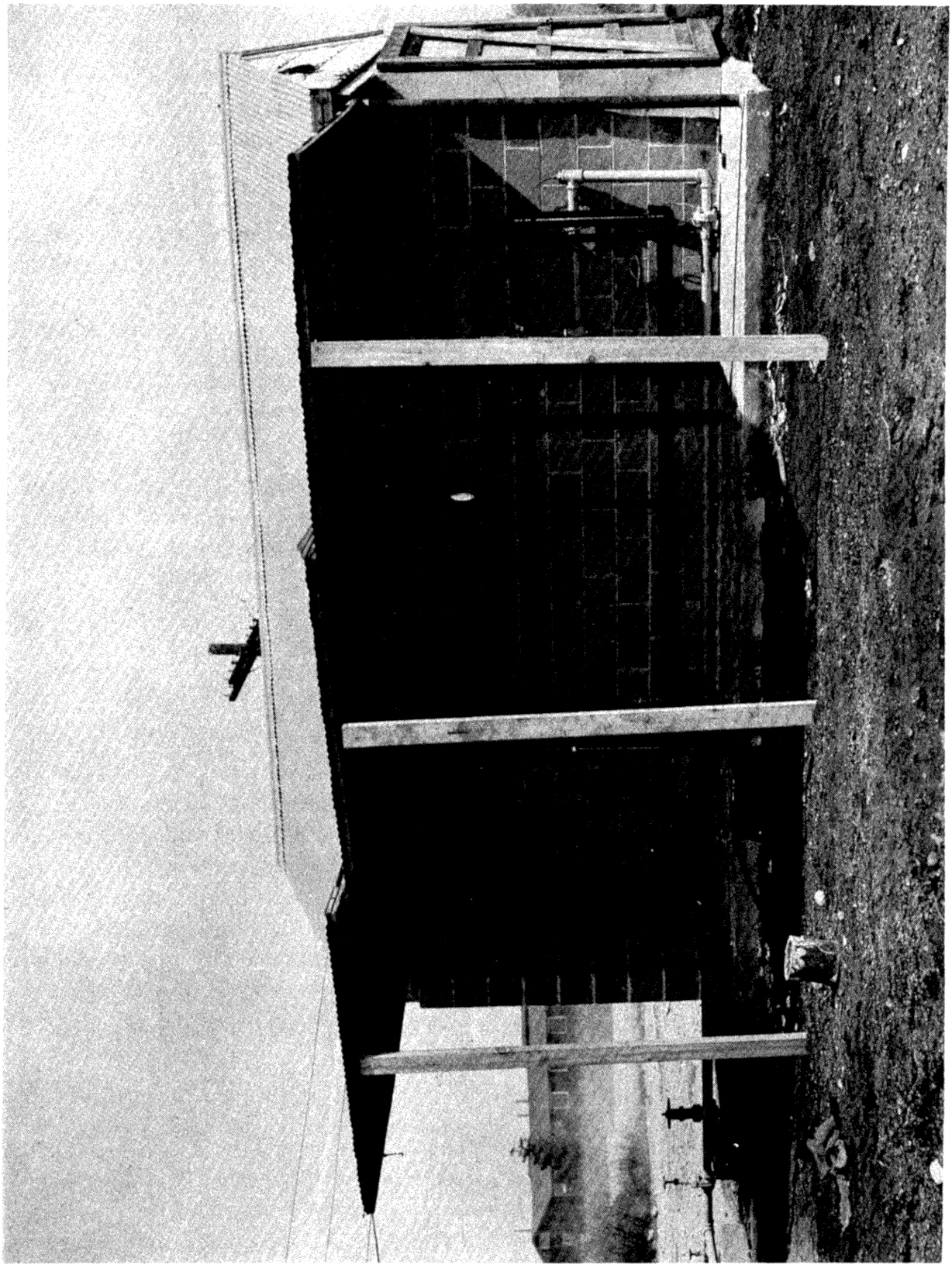

FIG. 11 OUTSIDE VIEW OF TEST STAND

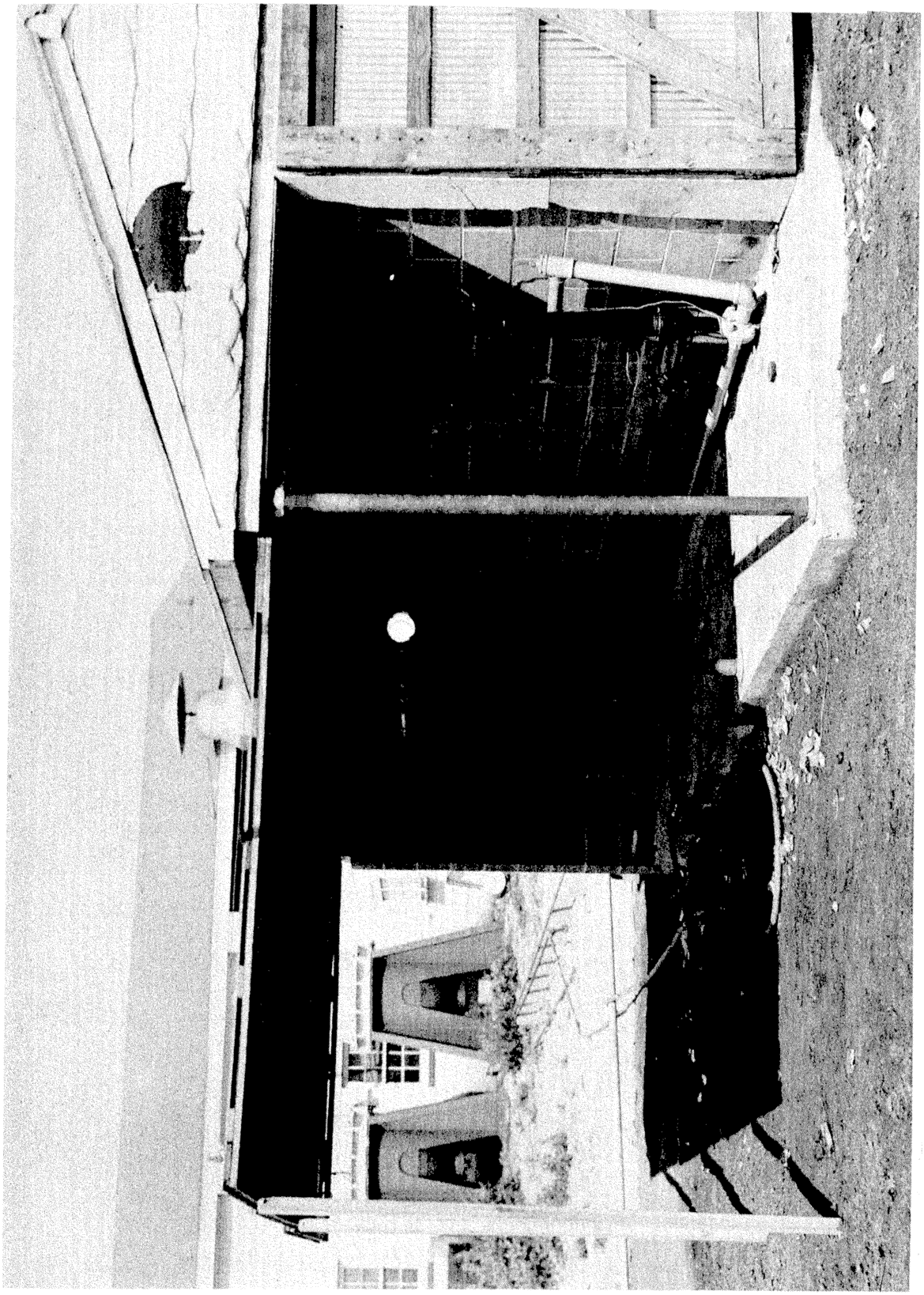

FIG. 12 OUTSIDE VIEW OF TEST STAND

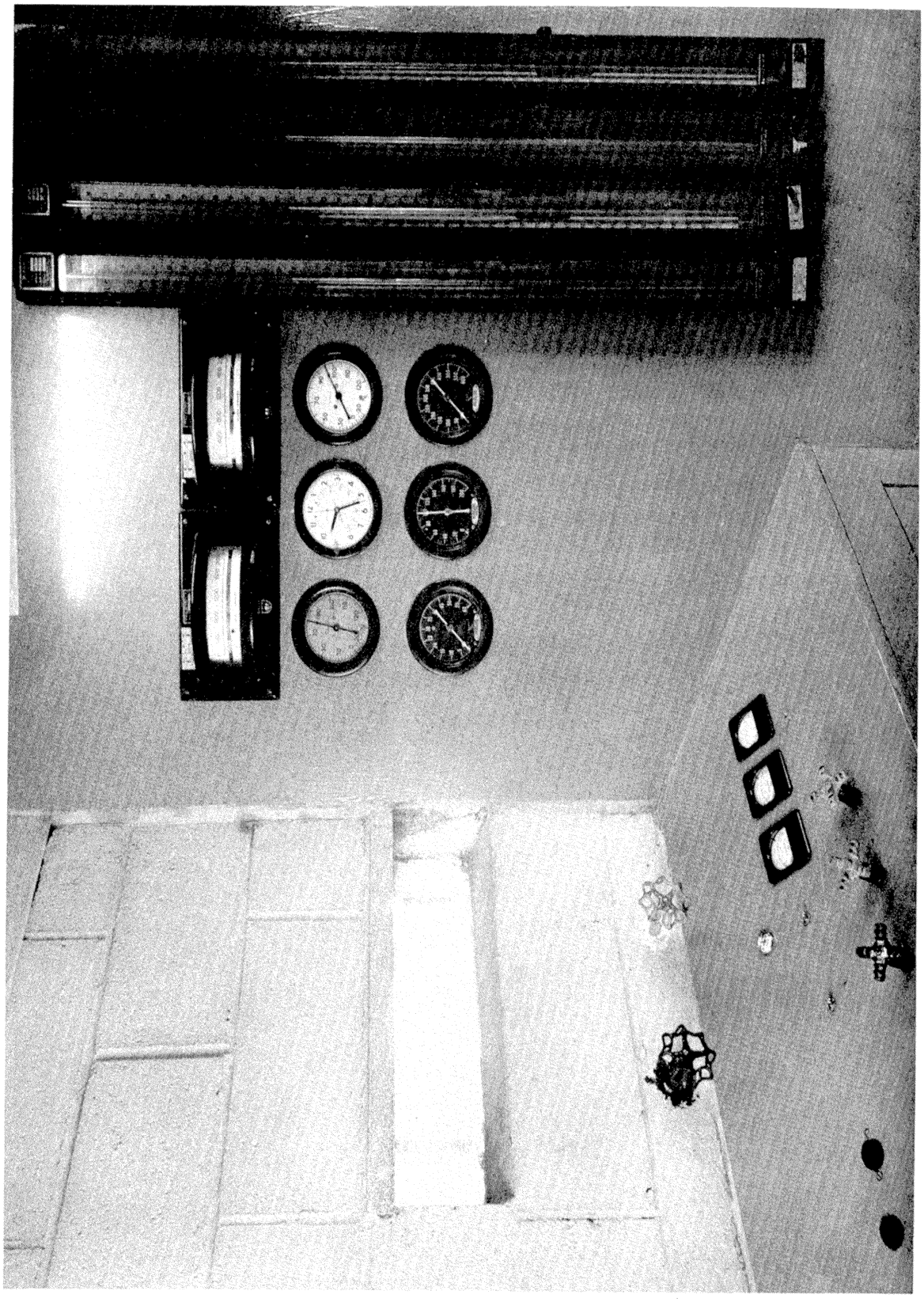

FIG. 13 CONTROL PANEL FOR TEST STAND

the conditions of operation and was reduced slightly during operation because the propane temperature in the tank was lowered due to evaporation. The air and propane orifices were not calibrated after installation, as no facilities were available for calibrating them under conditions similar to operating conditions (10 lbs/sec of air at 500 psi and 1 lb/sec of propane at approximately 100 psi). For this reason, the mass flows were computed from the ASME orifice formulas. The writers have constructed other orifices according to ASME specifications and then calibrated them. The calibrations have agreed quite satisfactorily with the values predicted from the design curves. For this reason, it is believed that no appreciable error is involved because the orifices were not calibrated.

3. Burner Upstream Pressure

The burner upstream pressure was measured at a static pressure tap 3 inches upstream from the burner inlet with a 0-60 psi pressure gage.

4. Burner Wall Temperature

The temperature indicating instruments shown in figure 13 are Wheelco Model 14 Thermocouple Indicators Range 0-2000°F. The thermocouples were connected at points on the burner shell.

5. Ceramic Surface Temperature

The ceramic surface temperature at the exit of the burner was measured by a Leeds and Northrup Optical Pyrometer. During operation the burner was viewed through a 1.5 inch thick laminated glass observation window. Because of the possibility of the absorption of light by the window introducing an error in the optical pyrometer readings, a calibration was made. The temperature of the filaments of a tungsten filament bulb was measured by viewing the filament through the 1.5 inch glass with the pyrometer and then viewing the lamp through air alone. Thus a calibration curve was obtained over a temperature range of 2000-3500°F. At 3000°F, the temperature viewed through the window was approximately 50°F lower than the temperature obtained when the bulb was viewed through air alone. In figure 14 is shown a schematic diagram of the instruments and test equipment.

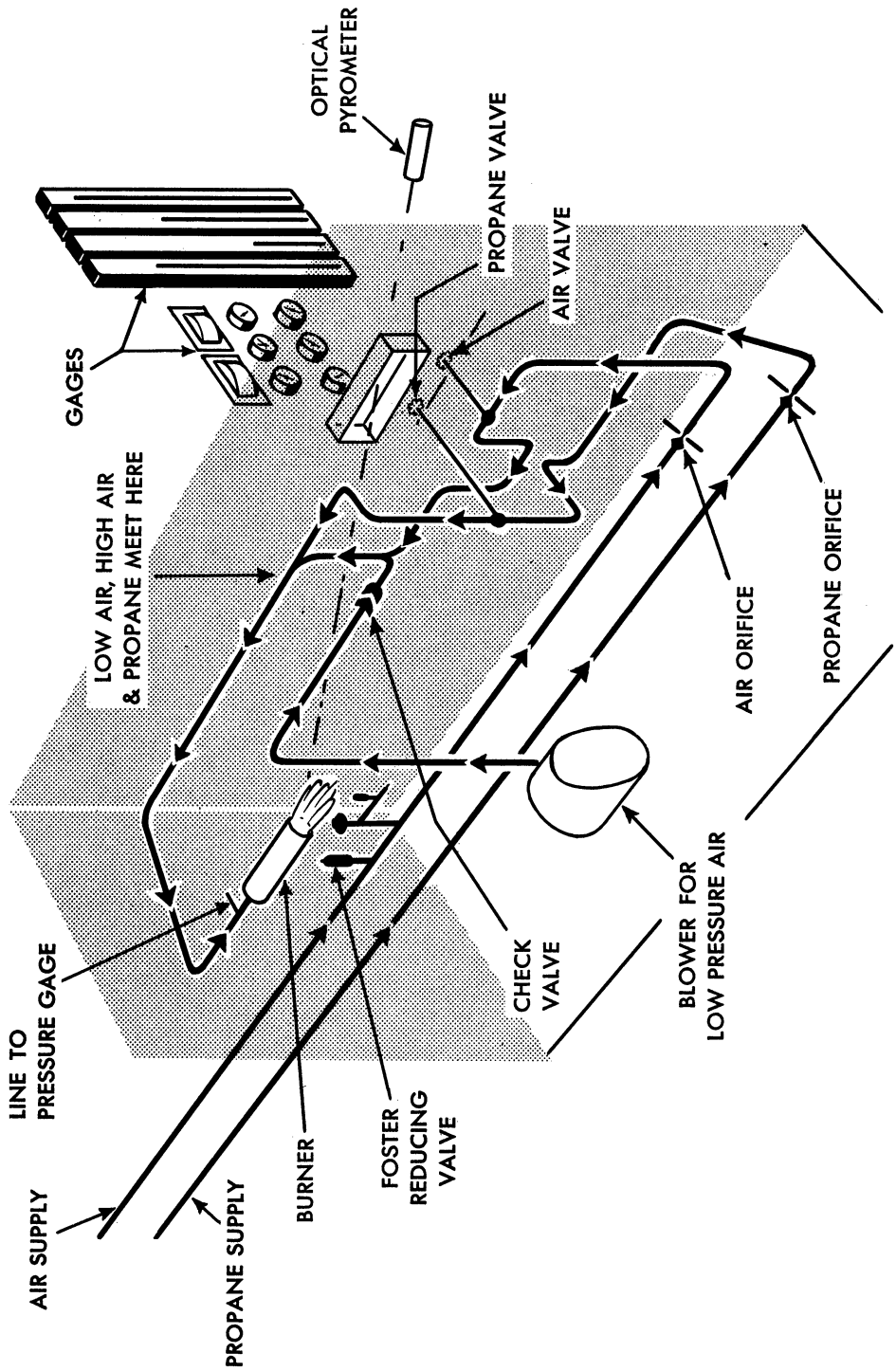


FIG. 14 SCHEMATIC DIAGRAM OF TEST EQUIPMENT

## IV. EXPERIMENTAL PROCEDURE

As was previously stated, there is no flame holder in these ceramic burners. The combustion chamber section has the same inside diameter as the pipe through which the fuel-air mixture is supplied. Since there is no flame holder, it is necessary to heat the ceramic surface somewhat before attempting to burn at high mass flow rate. This warm-up period is accomplished by operating the combustion chamber at relatively low flows for about five minutes. The air at low flow rates is supplied by a small turbo blower. When the ceramic surface has reached about 2500°F, high mass flows may be put through the burner without causing blowout. The testing technique used was as follows.

The air flow rate was adjusted to a predetermined value. This was done while maintaining the fuel-air ratio approximately stoichiometric. When the desired air flow rate was reached, the fuel-air ratio was changed over a range of values. At each fuel-air ratio rate, held constant for approximately 30 seconds, the following measurements were recorded--burner inlet pressure, ceramic surface temperature at exit, and the flow measurements (i.e., air and propane, pressure, temperature, and orifice pressured drop). Another air flow rate was then established and the process repeated. Burner lengths of 12, 15, 18, 24, and 30 inches were tested. Most of the runs were made on the 24 inch and 18 inch sections.

## V. CALCULATION OF PERFORMANCE FROM EXPERIMENTAL DATA

### A. Determination of Mass Velocity Through Burner

The flow measuring orifices were designed to ASME specifications. The flow formula[2] used is

$$w = 0.525\ KY\ D_o^2 \sqrt{\rho_o\ \Delta p_o} \qquad (1)$$

Mass velocity is defined as $G = w/A$, and the mass velocity through a three inch diameter burner may be found as follows. Substitute in equation (1) the appropriate values of the orifice diameter and the discharge coefficient[3] to obtain the following expressions for mass velocity:

For propane $$G_f = 1.00 \sqrt{\rho_o \Delta p}$$ lbs/sec/sq.ft. circular cross-sectional area (2)

For air $$G_a = 10.75 \sqrt{\rho_o \Delta p}$$ lbs/sec/sq.ft. circular cross-sectional area (3)

The air density was found from the pressure and temperature so measured by assuming that air behaved as an ideal gas. The value of the propane density was calculated from the expression $\rho_o = PM/ZRT$ using a molecular weight of 44 and obtaining values of the compressibility coefficient Z from published data[4] for pure propane at the pressure and temperatures measured. The fuel-air ratio ($G_f/G_a$) and the total mass velocity through the burner, ($G = G_f + G_a$) may be found from the measurements made of pressure, temperature and orifice pressure drop for the air and propane.

### B. Calculation of Minimum Mass Velocity Required for Mach at Exit = 1 Calculation of Exit Pressure at Higher Mass Velocities

At mass velocities below Mach = 1 at the exit, the exit pressure is assumed to be atmospheric. However, at mass velocities greater than that required for Mach = 1 at the exit, the velocity at the exit is equal to the velocity of sound, which, if ideal gases are assumed, may be expressed

as $C_s = \sqrt{\gamma\, gRT/M_w}$ ; hence the exit pressure may be computed by means of the conservation of mass, i.e.,

$$G = v\,\rho = \sqrt{\gamma\, g_c RT/Mw}\ \ (PMw/ZRT) \qquad (4)$$

Charts were prepared for the exit gas molecular weight as a function of fuel-air ratio and exit gas temperature, assuming equilibrium conditions. These compositions were obtained through the courtesy of Professor A. S. Foust, Department of Chemical Engineering, University of Michigan. Similar charts were prepared for values of $\gamma$ , as a function of fuel-air ratio and temperature, assuming equilibrium conditions. The values of $\gamma$ used for the pure components were obtained from Keenan and Kaye.[5]

The ceramic surface temperature at the exit of the combustion chamber was assumed to be equal to the stagnation temperature of the gas leaving the combustion chamber. By using equilibrium gas composition at a temperature calculated from the stagnation temperature, together with the mass velocity and considering the fact that the exit pressure is atmospheric for Mach numbers less than 1, it is possible to calculate the exit velocity and hence the exit Mach number by means of the relationship

$$\text{Mach No.} = \frac{\text{exit vel}}{\text{vel of sound at exit}} = \frac{G/\rho_s}{C_s} = \frac{GZRT/PMw}{\sqrt{\gamma\, g_c RT/Mw}} \qquad (5)$$

By means of equation (5), the mass velocity at which thermal choking (Mach = 1 at exit) first occurs for a stoichiometric mixture is found to be about 32 lb/sec/sq. ft. of combustion chamber cross-sectional area. Higher mass velocities will not change the inlet velocity or the exit Mach number, but will increase the pressure at the inlet and exit of the combustion chamber and hence allow more pounds of fuel to be burned per second if combustion is essentially complete in the burner. Calculated exit pressures (i.e., by substituting Mach = 1 into equation (5)) as high as 30 psia have been obtained.

C. Calculation of Combustion Chamber Parameter, $S_a$

The combustion chamber parameter $S_a$ has been previously described[1,6,7]. Briefly, it is derived as follows:

1. Conservation of momentum across a parallel wall duct established the following relation

$$A_2 P_2 (1 + \gamma M_2^2) - D_f = A_3 P_3 (1 + \gamma M_3^2) = F_3 \qquad (6)$$

2. From the energy and continuity equations, the following can be derived

$$F_3 = A_3 P_3 (1 + \gamma M_3^2) = \frac{C_s(1+f)\ (1+\gamma M_3^2)\left[2(\gamma+1)^{\gamma/2}\right]}{\gamma g_c M_3 \left(1 + \frac{\gamma-1}{2} M_3^2\right)\left[2(\gamma+1)^{1/2}\right]} \qquad (7)$$

3. Equation (7) can be written as a product of two independent parameter functions, Mach number and stagnation temperature, multiplied by the air flow rate

$$F_3 = W_a \left[\frac{C_s\ (1+f)\sqrt{2(\gamma+1)}}{\gamma g_c}\right]\left[\frac{1+\gamma \cdot M^2}{M\left(1 + \frac{\gamma-1}{2} M^2\right)^2 \sqrt{2(\gamma+1)}}\right] \qquad (8)$$

$$= W_a\ (S_a)(\phi M)$$

The $S_a$ term has been called the heat release or the specific air impulse by some investigators.[1] $S_a$ is dependent upon the stagnation temperature of the stream but since this can never be greater than the initial stagnation temperature plus the temperature effects of added heat, $S_a$ becomes a criterion of the amount of heat added, or in other words of the completeness of combustion for a given fuel-air mixture.

The $\phi M$ term which with $S_a$ makes up the stream thrust ($F/wa = (PA + mv/g_c)/w_a$) depends upon the exit Mach number. The exit Mach number is in turn limited by upstream and downstream conditions and is

fixed within these limits by the geometry of the burner. Thus $\phi$ M becomes a term that describes the physical characteristics of the burner that affect the gas flow and affect how well the heat of chemical reaction is converted to momentum in the exit gas. The preceding comments are based on considering a one dimensional flow. At Mach numbers at the exit equal to 1, $\phi M = 1$. Hence at Mach numbers at the exit less than 1, the stream thrust, $F/w_a$ is divided by $\phi$ M to obtain a value for $S_a$. This value of $S_a$ may be divided by the theoretical maximum value of $S_a$ to obtain a combustion chamber efficiency. With this method of evaluating combustion chamber efficiency, i.e., using $S_a$ instead of the stream thrust, the combustion chamber is penalized for any lack of uniformity of distribution in the exit flow. This is justifiable because the heat additions should be accomplished in such a way as to achieve maximum momentum increase and thereby provide the most thrust for a given energy addition. If the heat is added in such a manner that the flow is not uniformly distributed, the momentum increase of the flow is reduced. Since the combustion chamber is primarily utilized to produce thrust, a realistic combustion chamber efficiency should reflect a condition which detracts from the ultimate performance of the unit. In summing up, for Mach = 1, at the exit, $S_a$ is equal to the stream thrust, but for Mach numbers at the exit less than 1, the stream thrust is greater than $S_a$.

Equation (8) may be rearranged as follows

$$S_a = \frac{F}{wa\phi M} = \frac{PA+mv/g_c}{w_a \phi M} = \frac{PA + GAv/g_c}{\phi M \cdot GA/(1+f)} = \frac{P + \frac{G}{g_c} v}{\frac{G}{1+f} \phi M} \qquad (9)$$

The combustion chamber parameter, $S_a$, may be evaluated from experimental measurements made at either the exit or inlet of the combustion chamber by using equation (9) with the known value of the mass velocity, G. At the exit, for Mach numbers of 1, the exit pressure is calculated, as was previously shown, from the optical pyrometer temperature; the velocity is equal to the velocity of sound which is calculated from this temperature; and since Mach = 1, $\phi M = 1$. At Mach numbers less than 1, the exit pressure is assumed to be atmospheric, and the exit velocity and Mach number may be determined from the exit temperature. $\phi$ M is evaluated from a plot of $\phi$ M versus exit Mach number.[1]

At the inlet to the combustion chamber, the static pressure is measured. The pressure decrease between this point and the exit is due

to the sum of the pressure drop caused by burning and the friction loss in the combustion chamber. The friction loss in the chamber was found experimentally to be less than 1 psi over the flow ranges used (for cold flow) and was therefore assumed to be negligible compared to the 30-60 psia pressures obtained at the inlet to the combustion chamber. Since there is no flame holder in the chamber, the only friction loss is that due to the 15-24 inches of three inch pipe, and it seems reasonable that the pressure loss due to friction would be small.

At Mach numbers at the exit equal to 1, $\phi$ M = 1, the inlet velocity is constant, and consequently $S_a$ at the exit is determined by the inlet pressure measurement. At Mach numbers at the exit less than 1, the value of $\phi$ M was used as determined by the exit temperature measurements, but the pressure and velocity terms were determined from the inlet pressure measurements (since the friction loss is assumed to be negligible, the "stream thrust" is constant at any point in a straight pipe). Hence, two different values of $S_a$ were obtained at each point, one value based on the exit temperature, the other value based on the inlet pressure measurement. Inasmuch as these two values were close to one another, and inasmuch as either value is equally valid, the two values were arithmetically averaged.

## LIST OF ASSUMPTIONS

### DETERMINATION OF MASS VELOCITY THROUGH BURNER

1. The flow can be predicted by the use of the ASME orifice formulas.
2. The air at orifice conditions (500 psi approximately 60°F) is an ideal gas.

### CALCULATION OF EXIT PRESSURES

3. Gases at exit conditions (approximately 3000°F, 1 atmosphere) are ideal gases. Therefore

$$C_s = \sqrt{\gamma g_c RT/M_w}$$

and

$$Z = 1$$

4. The ceramic surface temperature at the exit of the combustion chamber is equal to the stagnation temperature of the exit gases.
5. The exit gas has the composition predicted for equilibrium conditions at the temperature and fuel-air ratios used.
6. At mass velocities such that the Mach number at the exit is less than 1, the exit pressure is atmospheric.

### DEVELOPMENT OF EXPRESSION FOR $S_a$

7. A cylindrical combustion chamber is employed, i.e. constant area burning.
8. No heat losses through the wall
9. Heating value of fuel is constant.
10. Use of arithmetical means of specific heats approximates results obtained by exact method for adiabatic compression or expansion
11. No friction losses in chamber

### CALCULATION OF $S_a$

All above assumptions which means stream thrust is constant at any point in the combustion chamber.

## TABLE OF NOMENCLATURE

$A = A_2 = A_3$ = Combustion chamber cross-sectional area, sq. ft.

$C_s$ = Velocity of sound = $\sqrt{\gamma\ g_c \frac{RT}{M_w}}$ if ideal gases are assumed

$D_o$ = Orifice diameter, inches

$D_f$ = Internal drag in combustion chamber due to friction loss at wall, assumed to be 0 in this case since no flame holder or other obstruction is present in the duct.

$f$ = fuel-air ratio, lb propane/lb air

$F_3$ = Stream thrust at exit of combustion chamber

$= P A + \frac{MV}{g_c}$

$g_c$ = Conversion factor for mass and force units = 32.2

$G_a$ = Air flow expressed as mass velocity - lbs. of air per sec. per sq. ft. of combustion chamber cross-sectional area

$G_f$ = Propane flow expressed as mass velocity lbs. of propane per sec. per sq. ft. of combustion chamber cross-sectional area

$G$ = Mass velocity through combustion chamber, lbs/sec/sq.ft. of combustion chamber cross-sectional area

$= G_a + G_f = v\rho = \frac{m}{A}$

KY = orifice coefficient[3]

$M_{w_o}$ = Molecular weight at orifice
Assumed equal to 44 at propane orifice
Assumed equal to 29 at air orifice

$M_w$ = Average molecular weight of exit gases; assumed equal to the molecular weight of a gas whose composition is determined by equilibrium conditions for exit temperature and fuel-air ratio used

M = Mach number = $\frac{\text{exit velocity}}{\text{velocity of sound at exit conditions}}$

TABLE OF NOMENCLATURE (CONTINUED)

$\phi M$ = Mach number function

$$= \frac{1 + \gamma M^2}{M\left(1 + \frac{\gamma - 1}{2} M^2\right)^{1/2} \sqrt{2(\gamma + 1)}}$$

= 1 when M = 1

m = total mass flow through burner, lb/sec

$= W_a + fW_a = GA$

$P_2$ = Pressure at inlet of combustion chamber, psia

$P_3$ = Pressure at exit of combustion chamber, psia

= Atmospheric pressure for Mach numbers less than 1, greater than atmospheric pressure for Mach exit = 1

P = Pressure, lbs per sq in absolute

$\Delta P_o$ = Pressure drop across orifice, lbs force per sq in

R = Universal gas constant

$S_a$ = Combustion chamber parameter = $\frac{C_s (1+f) \sqrt{2(\gamma+1)}}{\gamma g_c} = \frac{F}{W_a \phi M}$

$T_s$ = Ceramic surface temperature at exit measured by optical pyrometer assumed to be equal to stagnation temperature of exit gases $^{o}R$.

T = Average temperature of exit gases $^{o}R$

$= T_s \left(1 + \frac{\gamma - 1}{2} M^2\right)$

v = Linear velocity, ft/sec

$W_a$ = Mass flow of air, lb/sec

$W_o$ = Mass flow through orifice, lb/sec

Z = Compressibility factor

= 1 if ideal gases are assumed

$\gamma$ = ratio of specific heats; assumed to be equal to the $\gamma$ for a gas whose composition is determined by equilibrium condition for the temperature and fuel-air ratio used

$\rho_o$ = Density at orifice conditions, lbs mass/cu ft

$\rho_3$ = Density, lbs mass/cu ft at exit conditions

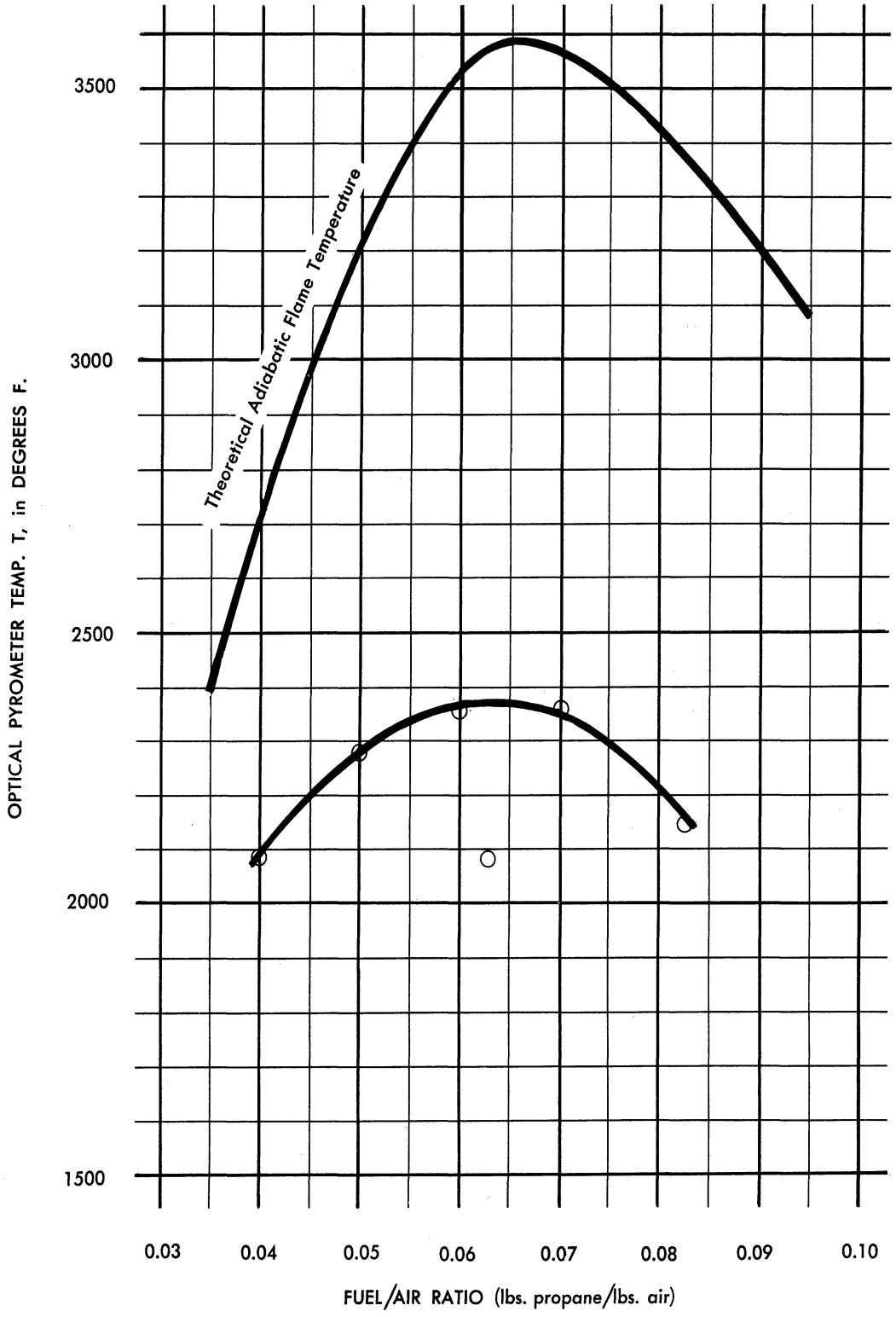


FIG. 15 PLOT OF OPTICAL PYROMETER TEMPERATURE VS. FUEL / AIR RATIO FOR 12 IN. CERAMIC BURNER, - 3 IN. DIA.

# VI. EXPERIMENTAL DATA

## A. Temperature Measurements

The temperatures shown in the following graphs are those temperatures obtained with the optical pyrometer, $T_p$, before correction for the absorption of the 1.5 inch thick glass observation window. These are the original points recorded, not the exit wall temperature, Ts, nor the exit gas temperature, T. The ceramic surface temperature, $T_s'$, may be obtained in degrees F, from the optical pyrometer temperature Tp by means of the equation resulting from the calibration made, i.e.,

$$T_s' = 1.050\ T_p' + 20 \quad (T \text{ in degrees Fahrenheit})$$

This equation is valid from 2300° to 3500°F.

The exit temperature of the gases, T, may be obtained from the ceramic surface exit temperature, Ts (in degrees Rankin, Ts = T's + 460) by the equation

$$T = Ts\ \left(1 + \frac{\gamma - 1}{2} M^2\right) \quad \left[T \text{ in degrees Rankin}\right]$$

The adiabatic flame temperature shown on the curves was obtained from a chart presented by Morrison and Dunlap.[8] These values were originally computed by Professor A. S. Foust, of the Chemical Engineering Department.

The experimental data obtained with the 12 inch long burner (Burner No. 3) is shown in figure 15, where the optical pyrometer temperature Tp is plotted against fuel-air ratio. The theoretical flame temperature is also shown for comparison. Figure 16 is a similar curve for the 15 inch long burner, except that two mass velocity ranges are shown, a high and low range.

Figures 17 and 18 show the experimental data obtained with the 18 inch long burner at four different mass velocity ranges, while in figure 19 this data is compared with the theoretical flame temperature. Figure 20 shows the data obtained with the 24 inch long burner.

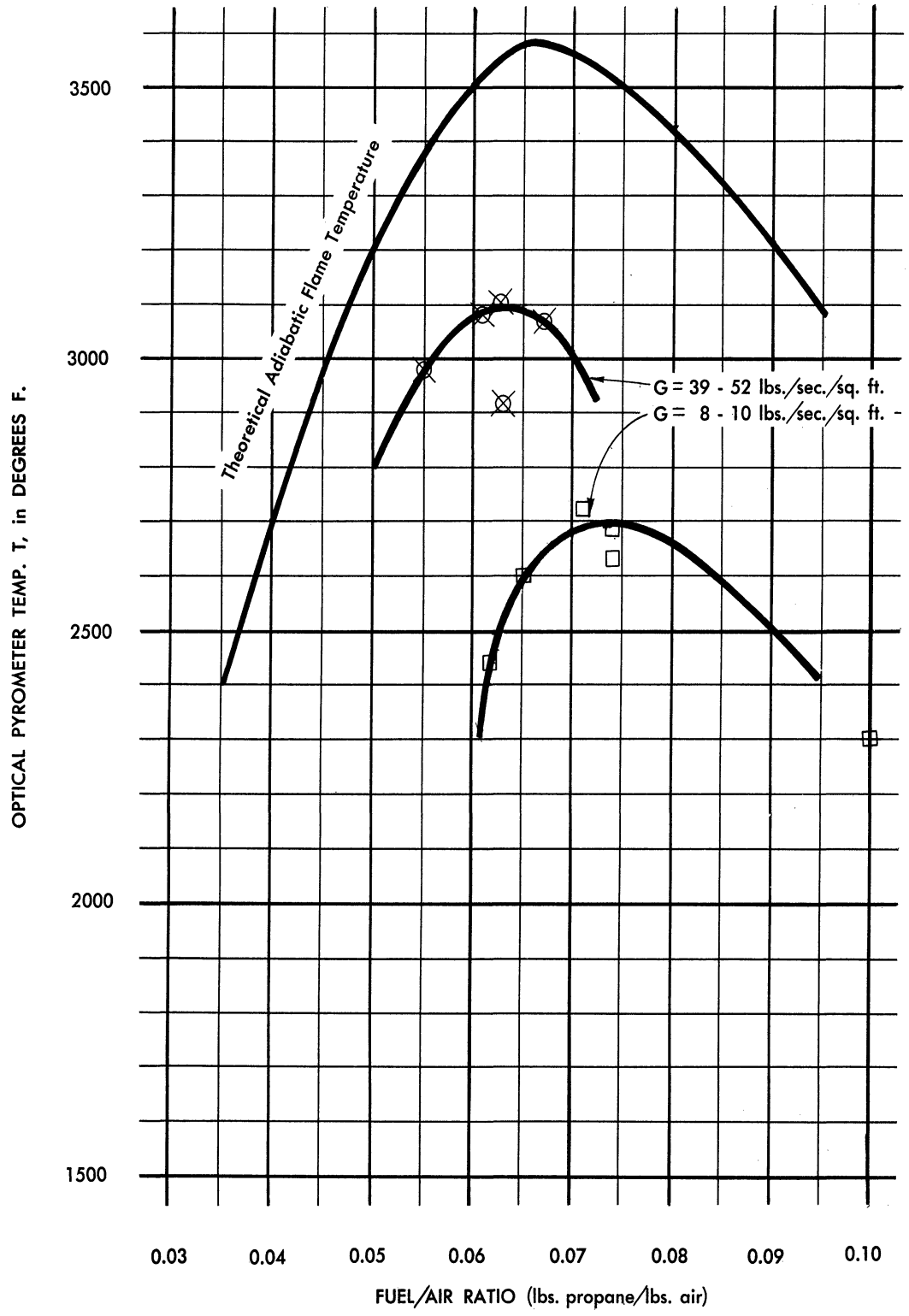


FIG. 16 PLOT OF OPTICAL PYROMETER TEMPERATURE VS FUEL/AIR RATIO FOR 15 IN. CERAMIC BURNER, - 3 IN. DIA.

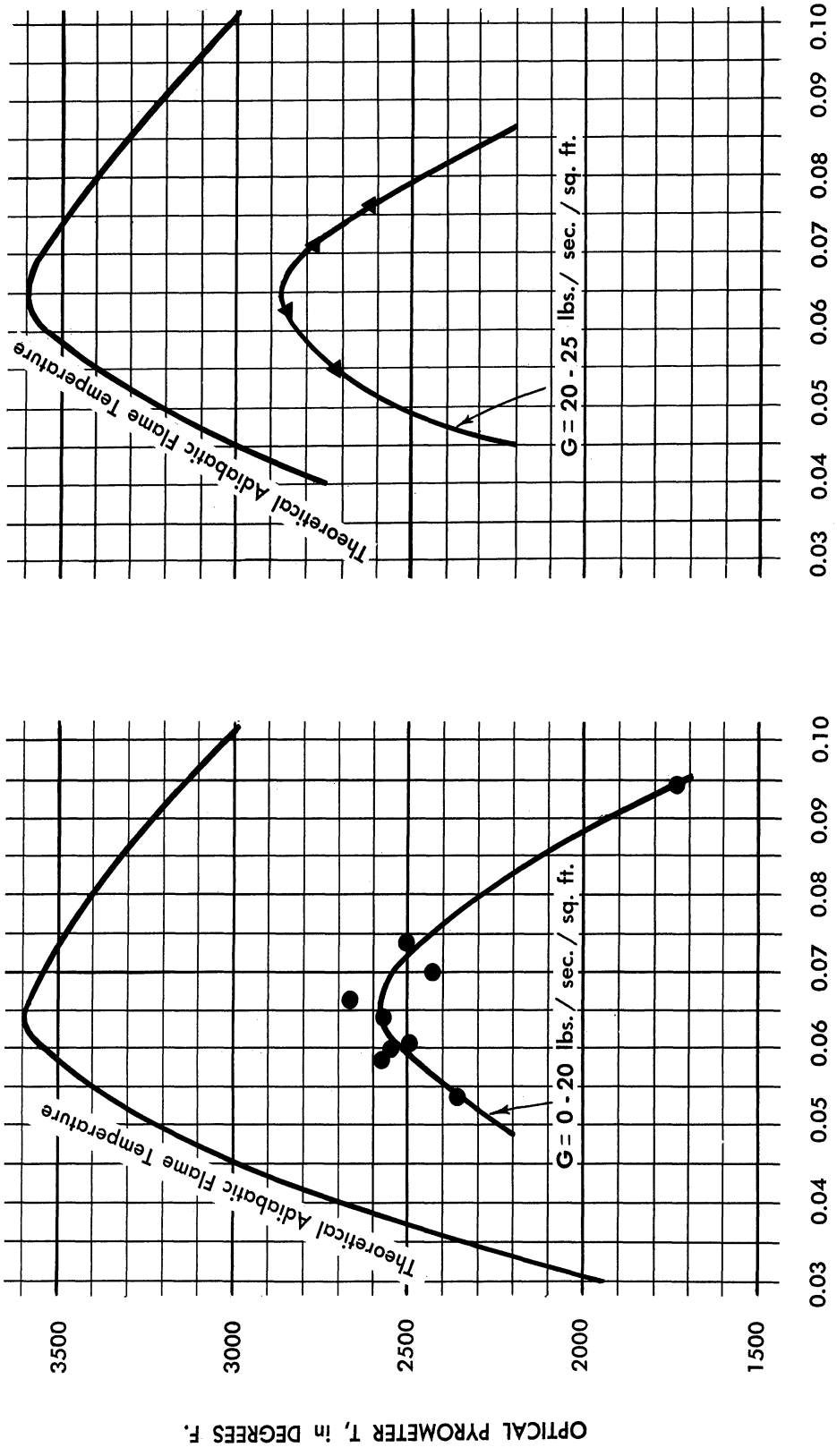


FIG. 17 PLOT OF OPTICAL PYROMETER TEMPERATURE VS FUEL/AIR RATIO FOR 18 IN. CERAMIC BURNER, - 3 IN. DIA.

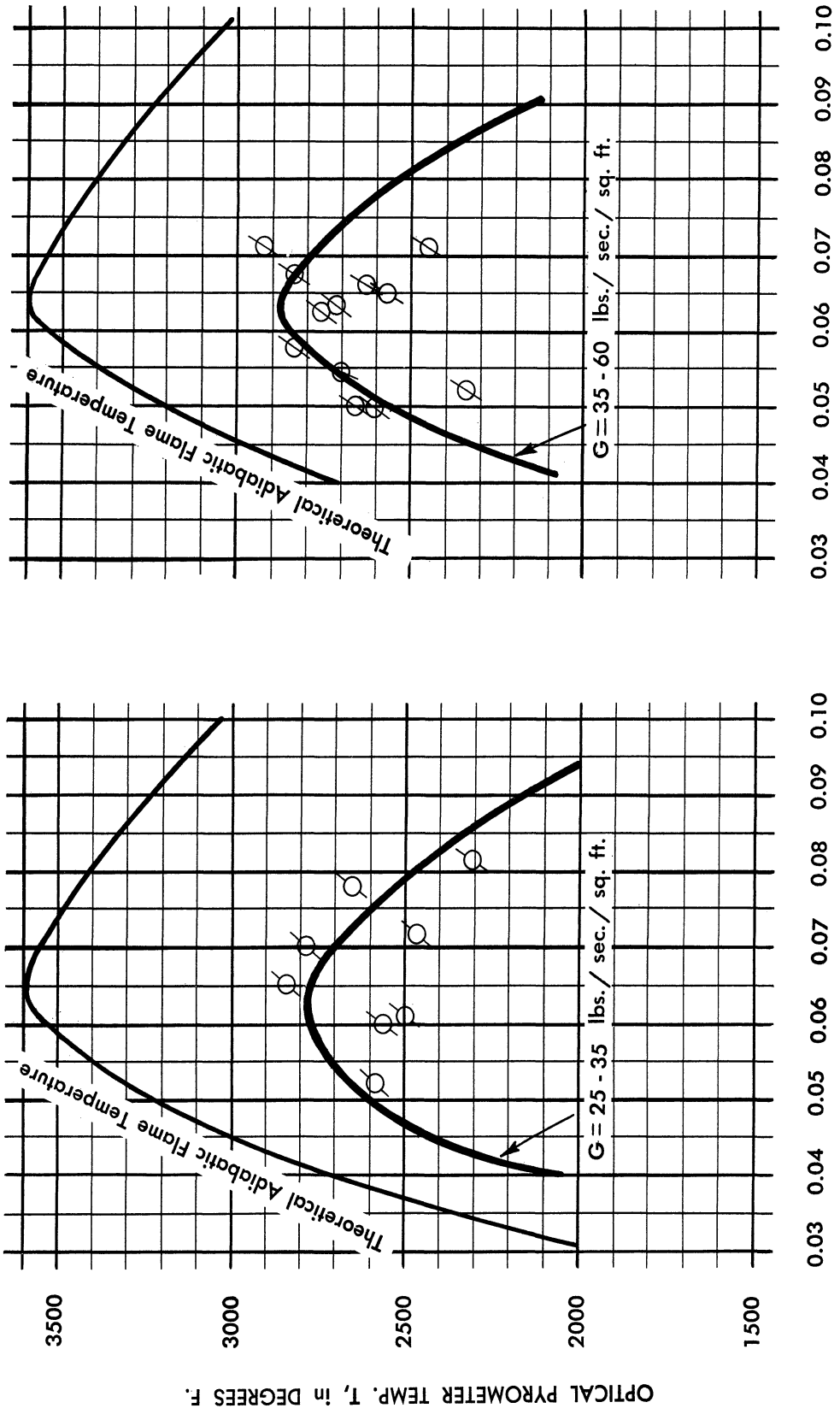


FIG. 18 PLOT OF OPTICAL PYROMETER TEMPERATURE VS. FUEL/AIR RATIO FOR 18 IN. CERAMIC BURNER, - 3 IN. DIA.

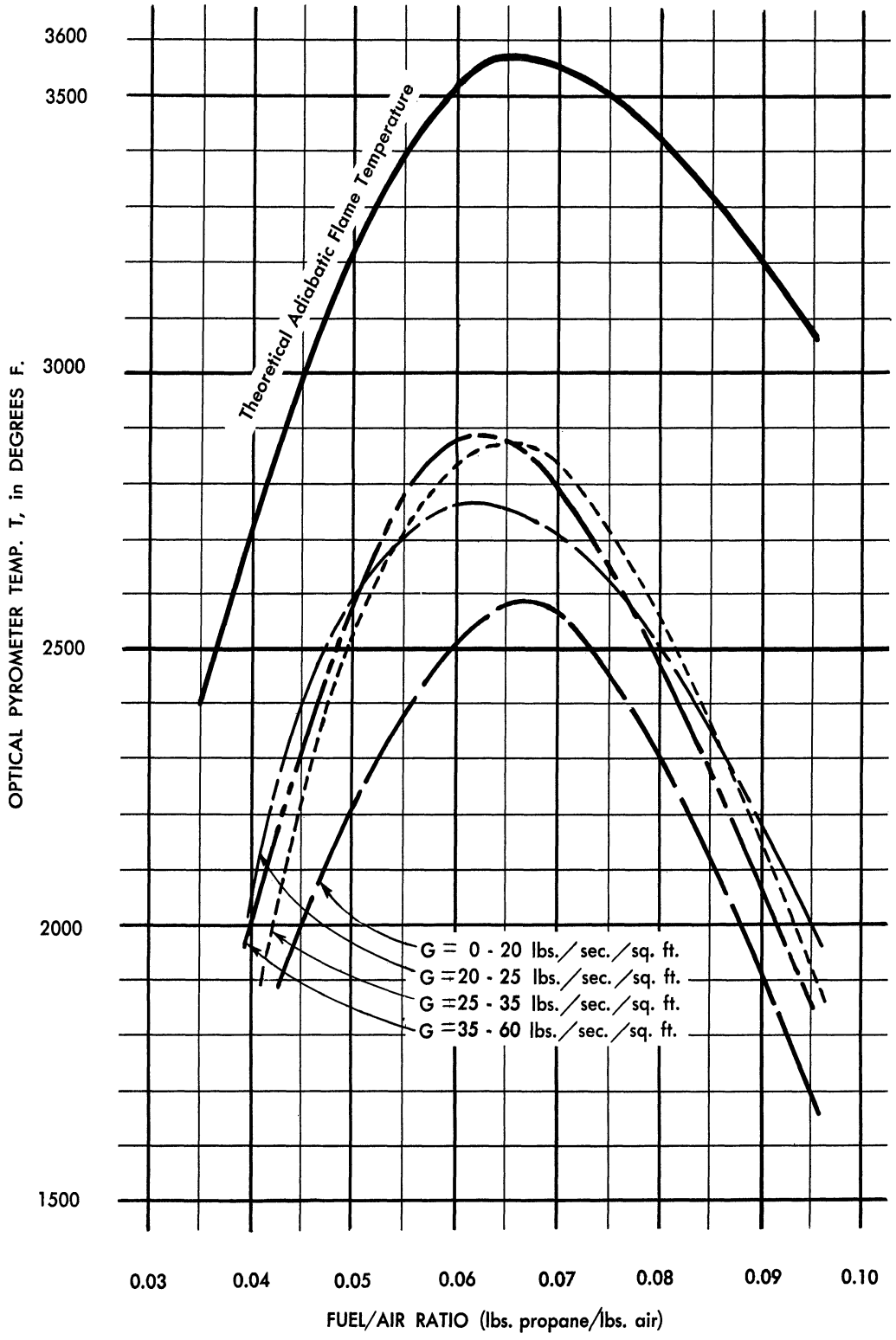


FIG. 19 PLOT OF OPTICAL PYROMETER TEMPERATURE VS. FUEL / AIR RATIO FOR 18 IN. CERAMIC BURNER, - 3 IN. DIA.

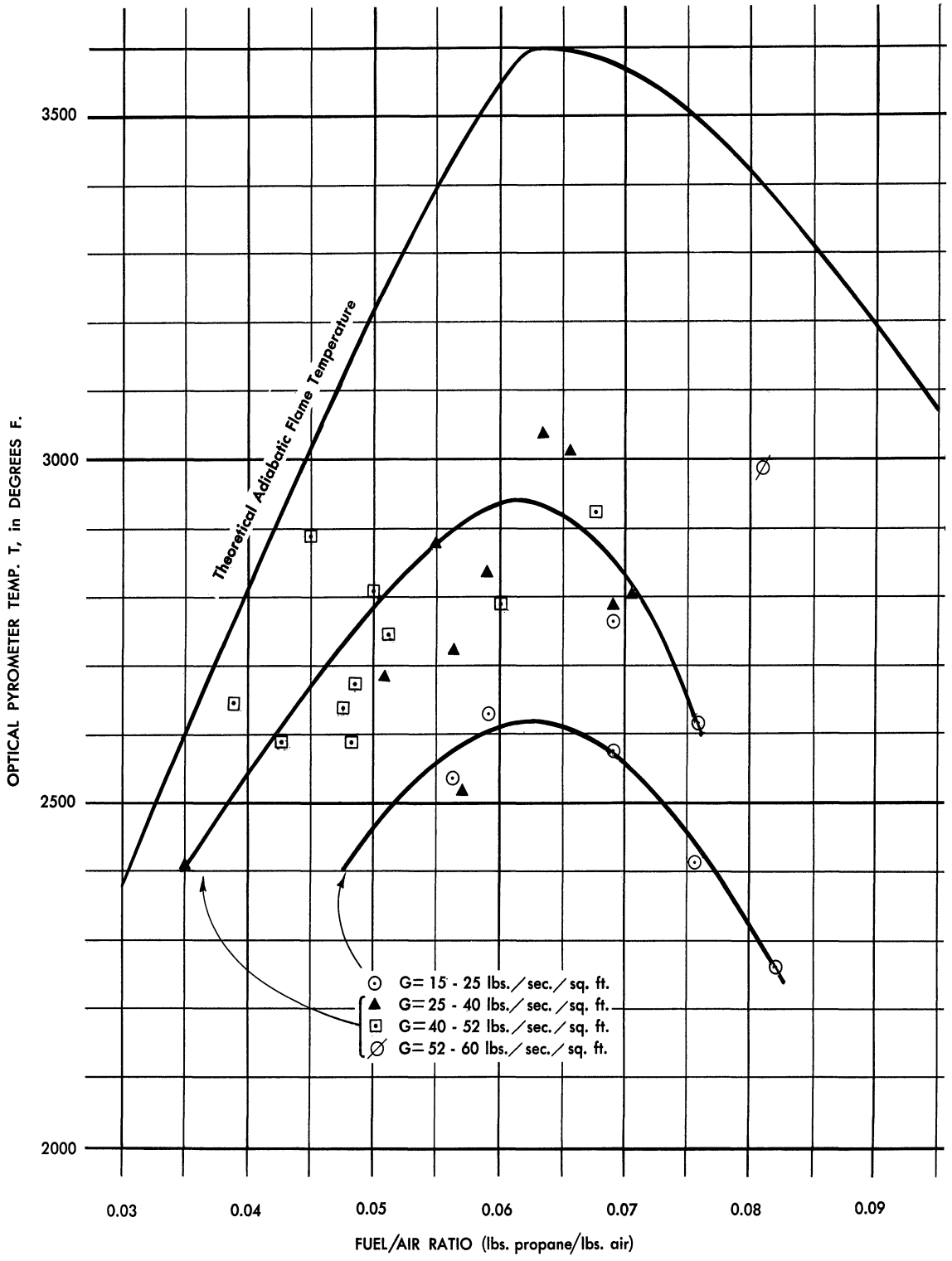


FIG. 20 PLOT OF OPTICAL PYROMETER TEMPERATURE

24 IN. CERAMIC BURNER, - 3 IN. DIA.

B. Inlet Pressure

The inlet pressures are plotted versus mass velocity in figure 21 and 22. Figure 21 shows the data for an 18 inch long burner, while figure 22 is for a 24 inch long burner. Since the mass velocity was relatively low for the 12 inch long burner, the gage pressure was 0 psia for all of the experiments performed with this burner. Insufficient data was obtained with the 15 inch long burner, at one fuel-air ratio, so that this data was not plotted.

C. Combustion Chamber Parameter, $S_a$

Except where otherwise noted, the value of $S_a$ shown on the following graphs was obtained by an arithmetical average of the $S_a$ calculated from the exit temperature measurements and the $S_a$ obtained from the inlet pressure measurement. The theoretical curves for $S_a$ shown on the various charts were obtained for propane-air mixtures by modifying an $S_a$ curve for gasoline-air mixtures.[1] A single calculation indicated that the $S_a$ for a stoichiometric gasoline-air mixture was equal to the $S_a$ for a stoichiometric gasoline-air mixture. The two curves would then be expected to have the same shape except that the propane-air $S_a$ curve would be shifted to the left of the gasoline-air $S_a$ curve. The amount of the shift is equal to the difference in the stoichiometric fuel-air ratios and is shifted along the fuel-air axis. To find a point on the propane-air curve, multiply the value of a point on the gasoline-air curve by the stoichiometric fuel-air ratio. This ratio is

$$\frac{.0665 \text{ propane-air}}{.0637 \text{ gasoline-air}} = 1.045$$

Thus for a fuel-air ratio of 0.05, the gasoline-air $S_a$ = 156; the propane-air $S_a$ = 156 x 1.045 = 163.

In figure 23 is shown the data obtained with the use of the 12 inch long ceramic burner at a low mass velocity (approximately 16 lb/sec/sq.ft.). With this burner length, it was not possible to burn at much higher mass velocities because of blowout. The data is shown as a plot of $S_a$ versus fuel-air ratio, compared to the theoretical maximum $S_a$.

In figure 24 is shown the data obtained with a 15 inch long burner. As may be seen, two mass velocity ranges are shown, a low range, approximately 8 and a high range, approximately 40 lbs/sec/sq.ft. of

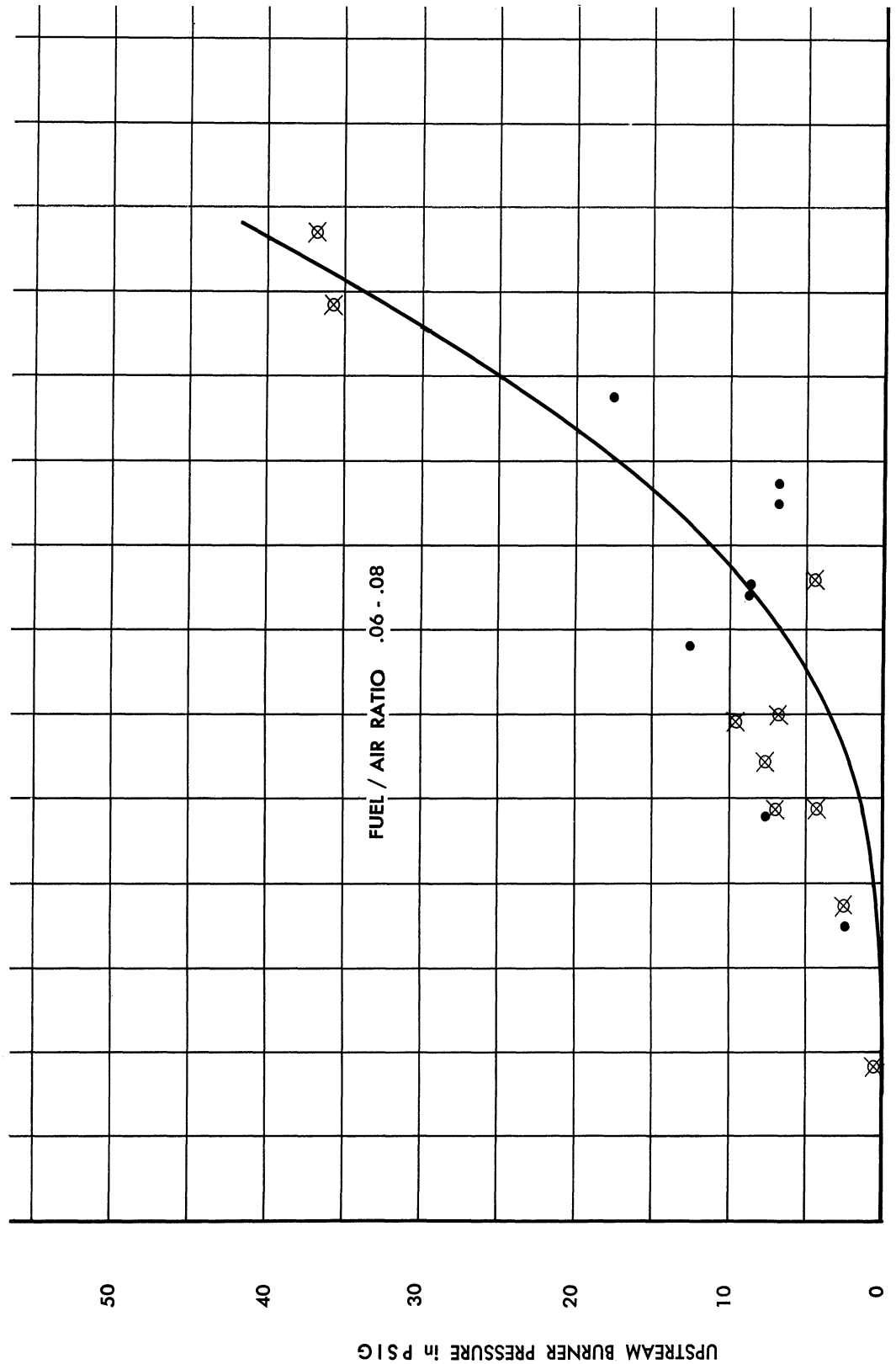


FIG. 21 UPSTREAM BURNER PRESSURE VS. MASS VELOCITY FOR 18 IN. CERAMIC BURNER, - 3 IN. DIA.

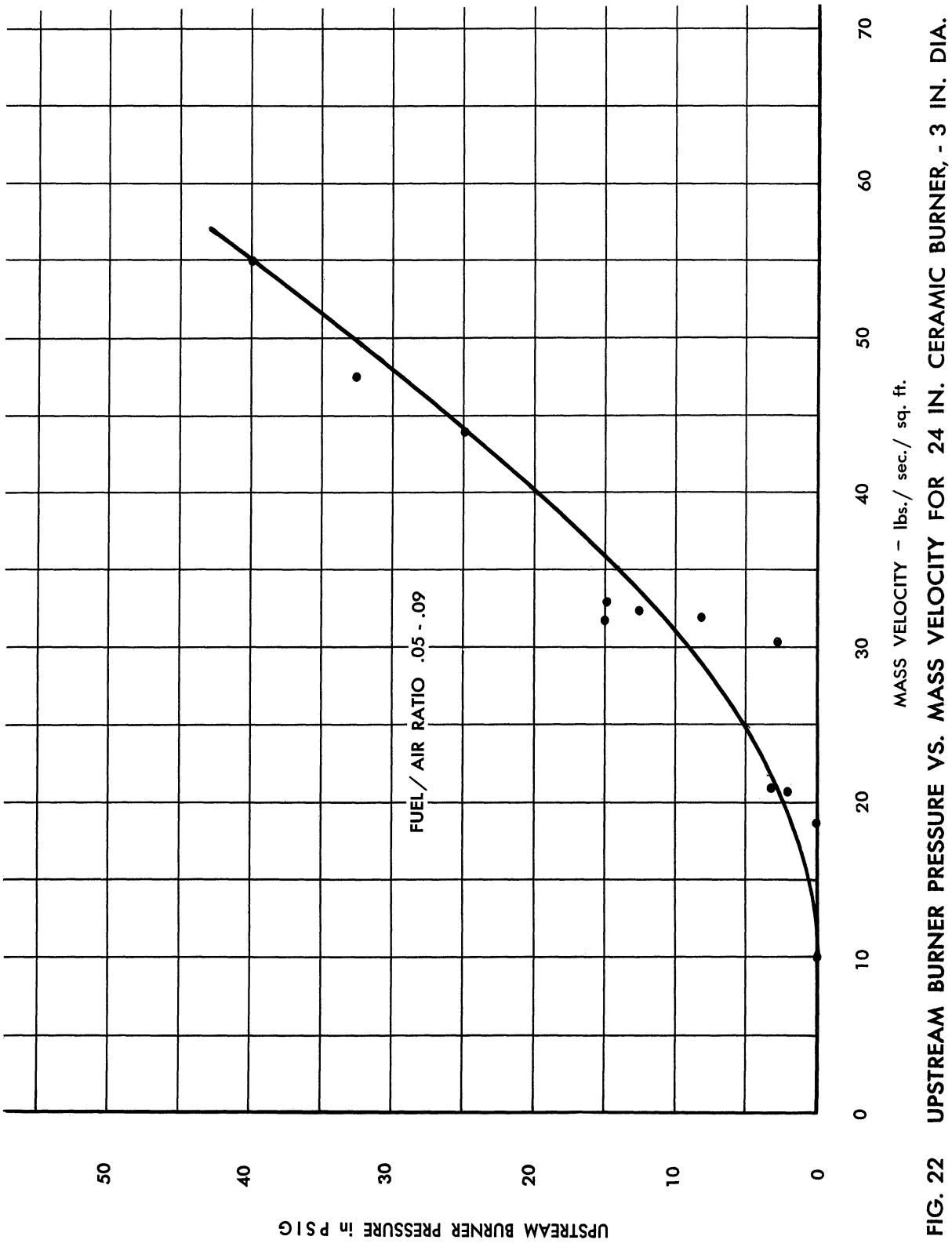


FIG. 22 UPSTREAM BURNER PRESSURE VS. MASS VELOCITY FOR 24 IN. CERAMIC BURNER, - 3 IN. DIA.

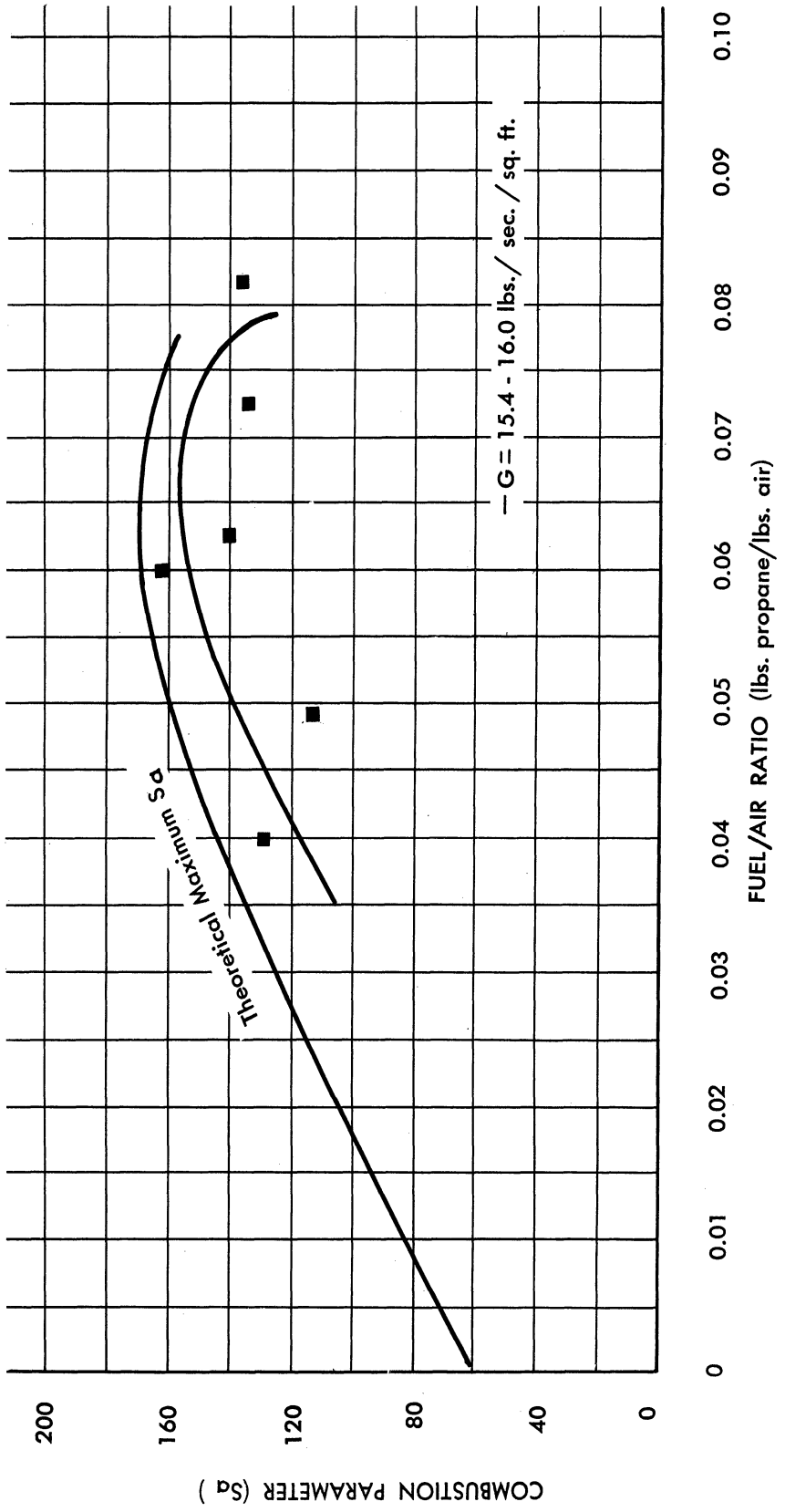


FIG. 23 COMBUSTION PARAMETER ($S_a$) VS. FUEL / AIR RATIO FOR 12 IN. CERAMIC BURNER, - 3 IN. DIA.

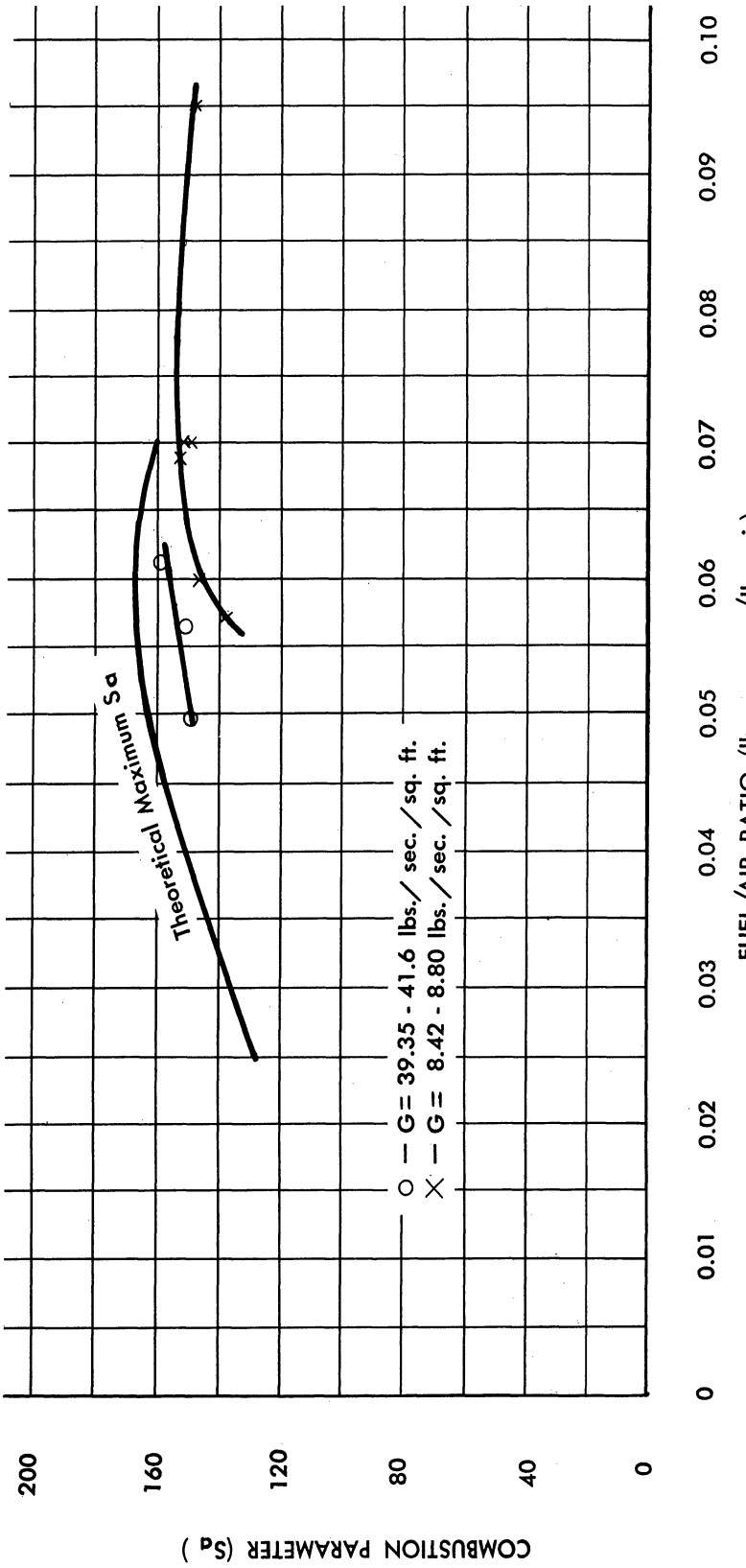


FIG. 24 COMBUSTION PARAMETER ($S_a$) VS. FUEL / AIR RATIO FOR THE 15 IN. LONG CERAMIC BURNER

combustion chamber cross-sectional area. It was possible to burn the 15 inch long burner at somewhat higher mass velocities than indicated, but no data was recorded then.

There was not a great deal of difference between the data obtained in the 18 inch long burner, and the data obtained with the 24 inch long burner. Consequently the data for the two burners are shown on figures 25, 26, and 27. Figure 25 is a plot of $S_a$ versus F/A for an intermediate mass velocity, figure 26 for a mass velocity just under thermal choking, and figure 27 is for a high mass velocity range. Some data was obtained at mass velocities as high as 60 lbs/sec/sq.ft., but insufficient points were recorded to obtain a complete curve. Some data was also obtained for burner lengths of 30 and 36 in. long, but insufficient data to draw curves was obtained, so this data is not presented.

D. Burner Length

There has not been enough data collected with different burner lengths to draw any conclusions concerning this point. At low mass velocities, the 12 inch burner length is reasonably efficient but will not maintain combustion at high mass flows. When the burner length is increased to 15 inches, blowout does not occur at mass flows greater than that required for thermal choking. The optimum burner length seems to be about 15 to 18 inches for a diameter of 3 inches. Shorter burners blow out while longer burners have a tendency toward rough burning. Although the efficiency of the 24 inch burner was about the same as that of the 18 inch burner, it appeared that the operation of the 18 inch length burner was a little smoother. Operation of the 36 inch length burner was extremely rough, making the recording of data difficult.

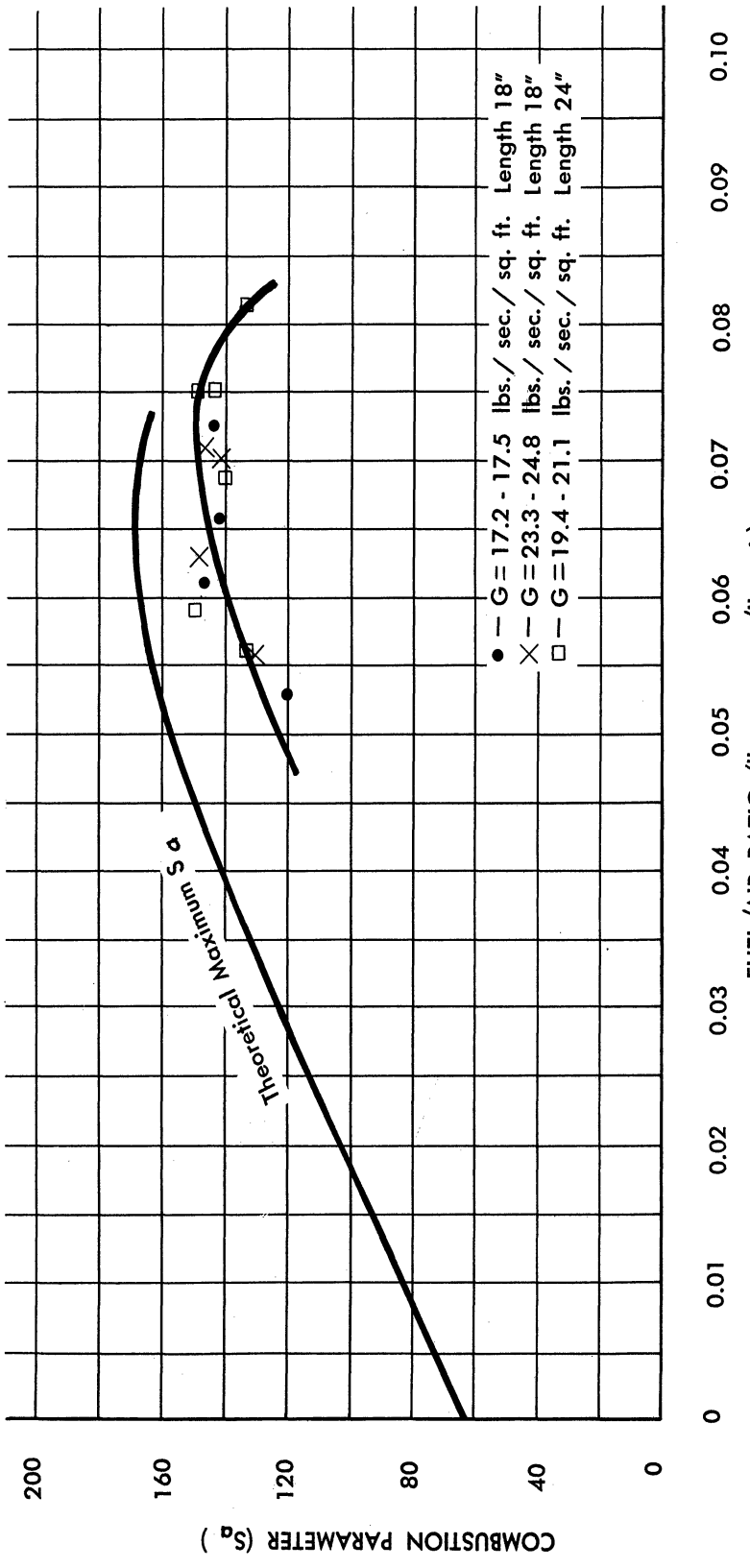


FIG. 25 COMBUSTION PARAMETER ($S_a$) VS. FUEL / AIR RATIO FOR INTERMEDIATE MASS VELOCITIES

CERAMIC BURNER, - 3 IN. DIA.

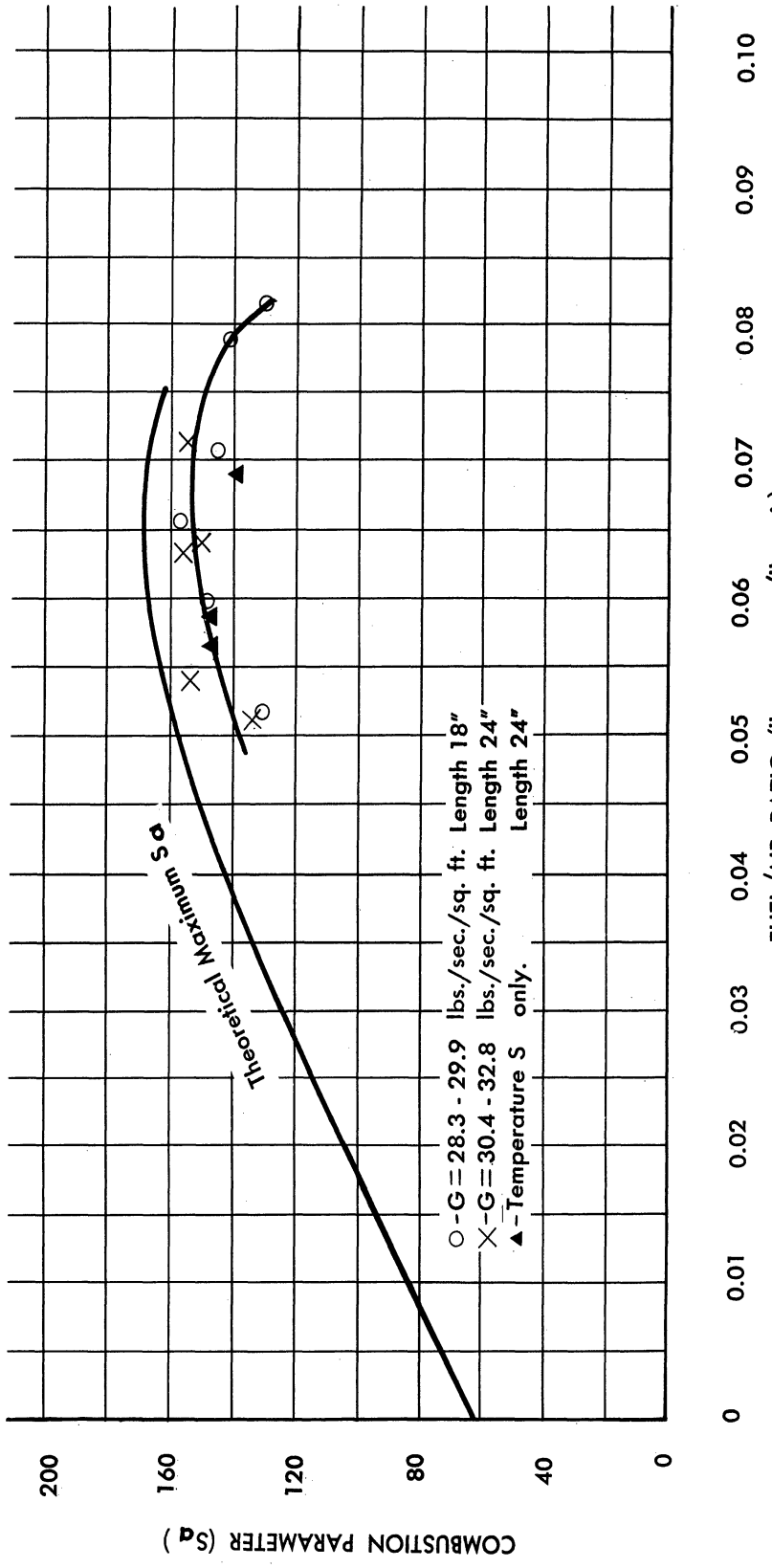


FIG. 26 COMBUSTION PARAMETER ($S_d$) VS. FUEL / AIR RATIO FOR MASS VELOCITIES JUST UNDER CHOKING. (M EXIT 0.90 - 0.95)

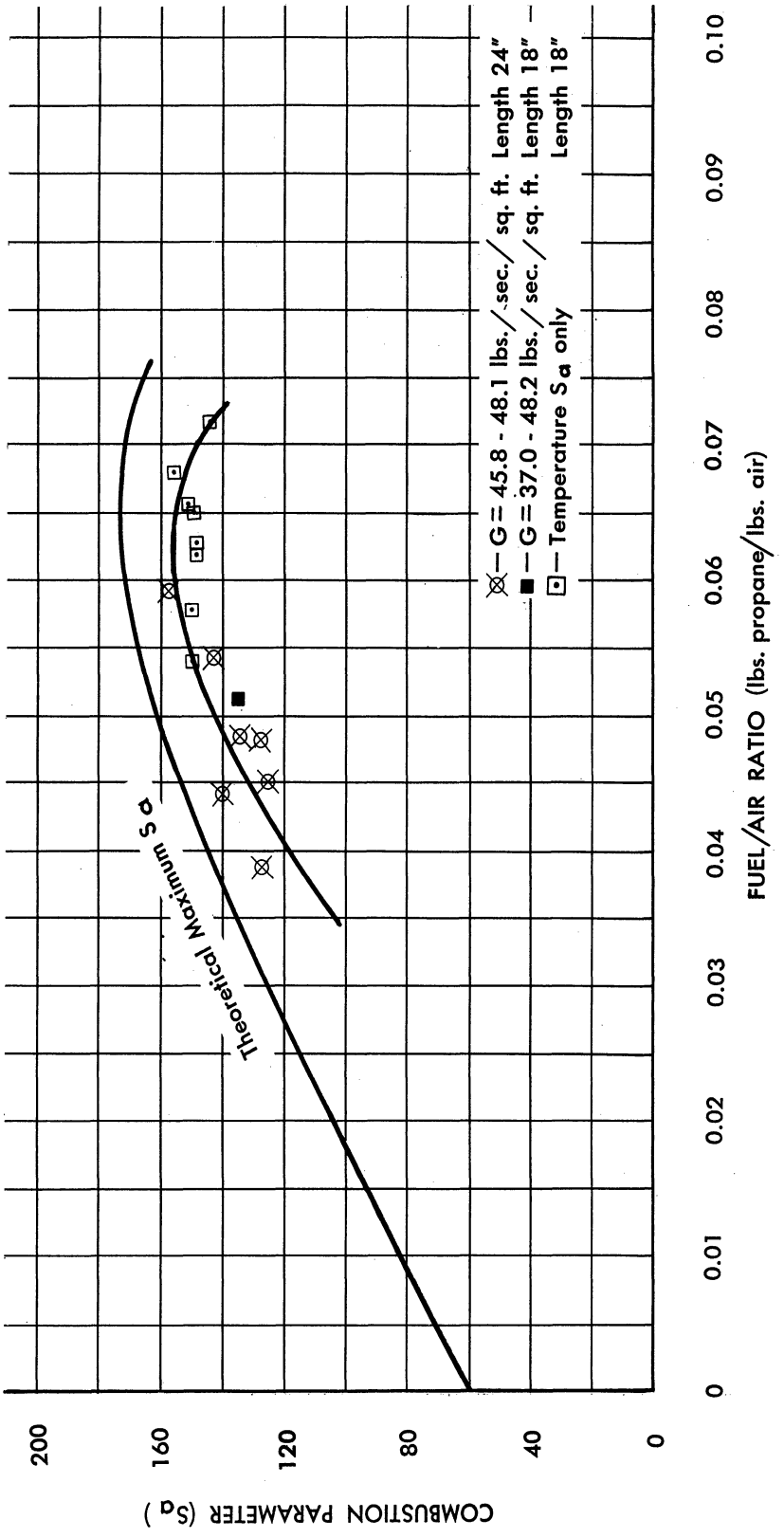


FIG. 27 COMBUSTION PARAMETER ($S_a$) VS. FUEL / AIR RATIO FOR MASS VELOCITIES IN EXCESS OF THAT REQUIRED FOR CHOKING. (3 IN. BURNER)

## BIBLIOGRAPHY

1 University of Michigan External Memorandum No. 7, "A Simplified Method of Calculating Ramjet Performance Applicable to High Mach Numbers," by J. R. Gannett, July 23, 1947.

2 Perry, "Chemical Engineer's Handbook," 3rd Edition, McGraw-Hill Book Co., New York, New York, 1950, page 404, equation 15b.

3 Ibid, page 405, figure 51.

4 Sage, et al., "Industrial and Engineering Chemistry," page 483, 1949.

5 J. H. Keenan and J. Kaye, "Gas Tables," John Wiley and Sons, New York, 1948.

6 University of Michigan Combustion Group Memorandum, November 30, 1949, by J. R. Gannett to E. T. Vincent, J. W. Luecht, and R. B. Morrison.

7 JHU/APL Bumble Bee Report No. 32, by T. Davis and J. R. Sellars, March 1946.

8 University of Michigan External Memorandum No. 21, "Measurement of Flame Speeds with the V-Flame," by R. B. Morrison and R. A. Dunlap, May 1948.

9 University of Illinois, Department of Ceramic Engineering, Report No. 17, 20, 26.

## DISTRIBUTION

Distribution of this report is made in accordance with AMC letter dated 8 April 1949.